RSC Advances

PAPER

View Article Online
View Journal | View Issue

Open Access Article. Published on 16 March 2015. Downloaded on 5/9/2026 9:53:25 AM.
This article is licensed under a Creative Commons Attribution-NonCommercial 3.0 Unported Licence.

Cite this: *RSC Adv.*, 2015, **5**, 27140

Stabilization of η^3-indenyl compounds by sterically demanding *N*,*N*-chelating ligands in the molybdenum coordination sphere†

Jakub Lodinský,[a] Jaromír Vinklárek,[a] Libor Dostál,[a] Zdeňka Růžičková[a] and Jan Honzíček*[b]

Received 24th January 2015
Accepted 11th March 2015

DOI: 10.1039/c5ra01450f

www.rsc.org/advances

A series of η^3-indenyl molybdenum compounds $[(\eta^3\text{-}4,7\text{-}Me_2C_9H_5)Mo(CO)_2(^{N,N}L)Cl]$ ($^{N,N}L$ = bpy, phen, pyma), isostructural with well-known η^3-allyl compounds, was synthesized from the recently established halide synthon $[\{(\eta^5\text{-}4,7\text{-}Me_2C_9H_5)Mo(CO)_2(\mu\text{-}Cl)\}_2]$. The low stability of the hexacoordinated η^3-indenyl molybdenum species in solution has been overcome by a modification of the chelating ligand. Hence, the dissociation of the compounds bearing ligands with methyl groups beside nitrogen donor atoms (*e.g.* 6,6′-Me_2-bpy, 2,9-Me_2-phen; 2,9-Me_2-4,7-Ph_2-phen) is strongly disfavored due to the steric requirements of the substituents. The considerable discrimination of the pentacoordinated species enables the use of $[(\eta^5\text{-}4,7\text{-}Me_2C_9H_5)Mo(CO)_2(2,9\text{-}Me_2\text{-phen})][BF_4]$ for the assembly of derivatives bearing other halides and pseudohalides in the coordination sphere of molybdenum. The current study further describes some other new indenyl complexes accessible from $[\{(\eta^5\text{-}4,7\text{-}Me_2C_9H_5)Mo(CO)_2(\mu\text{-}Cl)\}_2]$. All structural types presented in this experimental study were supported by X-ray crystallographic data.

Introduction

Organometallic molybdenum compounds are currently under comprehensive scrutiny due to their interesting properties. Allyl compounds $[(\eta^3\text{-}C_3H_5)Mo(CO)_2(^{N,N}L)Cl]$ ($^{N,N}L$ = *N*,*N*-chelating ligand) show a rich coordination chemistry and have found several applications in organic synthesis and catalysis.[1–11] Promising cytotoxic properties have been observed for cationic cyclopentadienyl and indenyl compounds $[(\eta^5\text{-}Cp')Mo(CO)_2(^{X,X}L)][BF_4]$ (Cp′ = Cp = C_5H_5, Ind = C_9H_7), where $^{X,X}L$ is *N*,*N*-, *P*,*P*- or *S*,*S*-chelating ligands, and their congeners with substituted π-ligands.[12–14] Neutral cyclopentadienyl compounds $[(\eta^5\text{-}Cp')Mo(CO)_3X]$ (Cp′ = substituted Cp, X = anionic ligand) are well-established precursors of catalysts for oxidation reactions (*e.g.* olefin epoxidation or sulfoxidation).[15–21] Recently, we have described a synthesis of $[\{(\eta^5\text{-}Ind)Mo(CO)_2(\mu\text{-}Cl)\}_2]$ (**1**; Scheme 1) that was found to be a versatile synthon for various η^3-indenyl compounds.[22] Furthermore, this compound seems to be a suitable pre-catalyst for isomerization of α-pinene oxide to campholenic aldehyde[23] and a precursor of hydrolytically active species for promoted hydrolysis of phosphoesters.[24]

Although the cyclopentadienyl and indenyl molybdenum compounds have often a similar molecular structure, a different reactivity is expected since a replacement of the cyclopentadienyl ligand with the indenyl accelerates reaction rates due to a lower energetic barrier of the haptotropic shift of the π-ligand.[25–29] The kinetic "indenyl effect" has been comprehensively scrutinized on various molybdenum compounds by Romão and Calhorda.[30–32] For instance, they have recently demonstrated that the indenyl compound $[(\eta^5\text{-}Ind)Mo(CO)_2(\kappa^2\text{-}ttcn)][BF_4]$ (ttcn = 1,4,7-trithiacyclononane) undergoes an acid-activated C–S cleavage to give $[(\eta^5\text{-}Ind)Mo(CO)\{\kappa^3\text{-}(SCH_2CH_2)_2S\}][BF_4]$, while the cyclopentadienyl analogue is stable under similar conditions.[33] An activation of coordinated ligand was also observed for complexes with η^4-bonded spiro-[2.4]hepta-4,6-diene. The cyclopentadienyl compound $[(\eta^5\text{-}Cp)$-

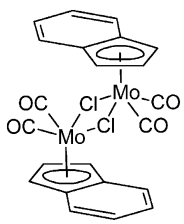

Scheme 1 Molecular formula of **1**.

[a]*Department of General and Inorganic Chemistry, Faculty of Chemical Technology, University of Pardubice, Studentská 573, Pardubice, Czech Republic*

[b]*Institute of Chemistry and Technology of Macromolecular Materials Faculty of Chemical Technology, University of Pardubice, Studentská 573, Pardubice, Czech Republic. E-mail: jan.honzicek@upce.cz; Fax: +420 46603 7068*

† CCDC 1044572–1044582. For crystallographic data in CIF or other electronic format see DOI: 10.1039/c5ra01450f

This journal is © The Royal Society of Chemistry 2015

Open Access Article. Published on 16 March 2015. Downloaded on 5/9/2026 9:53:25 AM.
This article is licensed under a Creative Commons Attribution-NonCommercial 3.0 Unported Licence.

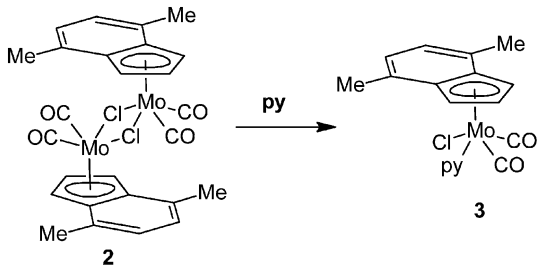

Scheme 2 Reaction of **2** with pyridine.

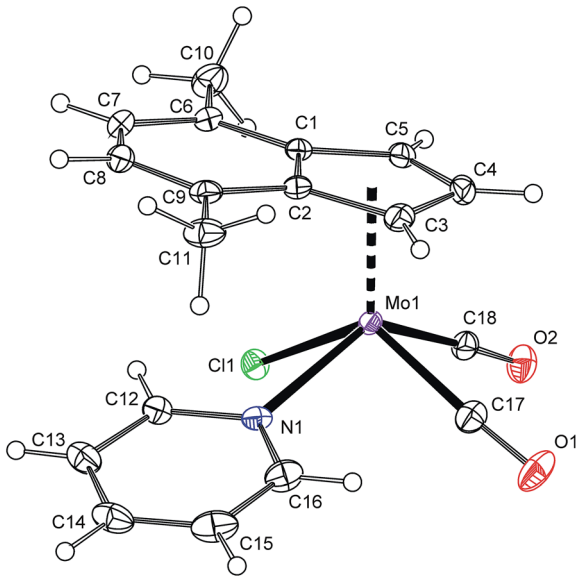

Fig. 1 ORTEP drawing of $[(\eta^5\text{-}4,7\text{-}Me_2C_9H_5)Mo(CO)_2(py)Cl]$ (**3**). The labeling for all non-hydrogen atoms is shown. Thermal ellipsoids are drawn at the 30% probability level.

$\{\eta^4\text{-}C_5H_4(CH_2)_2\}Mo(CO)_2][BF_4]$ is unusually stable, while the indenyl analogue undergoes a spontaneous and very fast ring-opening to $[(\eta^5\text{-Ind})(\eta^5\text{-}C_5H_4CH_2\text{-}\eta^1\text{-}CH_2)Mo(CO)][BF_4]$.[34,35]

The aim of this study is to bring a detail description of the coordination properties of $[\{(\eta^5\text{-}4,7\text{-}Me_2C_9H_5)Mo(CO)_2(\mu\text{-Cl})\}_2]$ (**2**) in attempt to synthesize new η^3-indenyl compounds structurally related with the well-known complexes bearing η^3-allyl $[(\eta^3\text{-}C_3H_5)Mo(CO)_2(^{N,N}L)Cl]$. It will be shown that a steric congestion of the chelating ligand is critical for the stability of $[(\eta^3\text{-}4,7\text{-}Me_2C_9H_5)Mo(CO)_2(^{N,N}L)Cl]$ and could be used for the control of the indenyl ring slippage. When this work was in progress, the first notes about reactivity of the parent compound **1** with coordinating solvents have appeared in literature[23,24] but the detailed description of the coordination behavior is still missing. Our current study deals with species bearing 4,7-dimethyl indenyl ligand mainly due to higher solubility of **2** in organic solvents.[22] This substitution pattern usually has only negligible effect on the reactivity due to subtle steric and electronic effects of two methyl groups in the C_6-ring.[36,37]

Results and discussion

Reactions of $[\{(\eta^5\text{-}4,7\text{-}Me_2C_9H_5)Mo(CO)_2(\mu\text{-Cl})\}_2]$ (2) with py, bpy, phen and pyma

Reaction of $[\{(\eta^5\text{-}4,7\text{-}Me_2C_9H_5)Mo(CO)_2(\mu\text{-Cl})\}_2]$ (**2**) with pyridine (**py**) gives a monomeric compound with η^5-bonded indenyl ligand $[(\eta^5\text{-}4,7\text{-}Me_2C_9H_5)Mo(CO)_2(py)Cl]$ (**3**), see Scheme 2. The expected η^3-indenyl species, which could appear upon coordination of further **py** molecule to molybdenum, was not detected even when a large excess of the reagent was used. Although the compound **3** is a structural analogue of the previously described cyclopentadienyl compound $[(\eta^5\text{-Cp})Mo(CO)_2(py)Cl]$,[38] the original route is not suitable for **3** due to a low stability of the indenyl precursor $[(\eta^5\text{-Ind})Mo(CO)_3Cl]$ at elevated temperature.[39]

^{1}H NMR spectrum shows the signal of H^2 at a high field that is typical for the species with η^5-coordinated indenyl ligand.[40] The spectrum pattern with magnetically inequivalent protons H^1 and H^3 imply the C_1 point symmetry for the molecule of **3** that is fully in agreement with the solid state structure revealed by single crystal X-ray analysis (Fig. 1 and Table 1). The molecule of **3** has a square pyramidal structure with the η^5-bonded indenyl ligand in the apical position. The basal plane is occupied with two *cis*-coordinated carbonyl ligands, one chloride and the nitrogen donor atom of pyridine. The η^5-coordination mode of the indenyl ligand is confirmed by a low value of the envelope fold angle [$\Omega = 7.4(2)^\circ$] and also by Δ(M–C) [0.212(2) Å].

From a mechanistic point of view, the η^5–η^3 rearrangement of the indenyl ligand is stimulated by a coordination of two 2e donors to molybdenum that could be further enforced by a chelating effect. Nevertheless, this process is further complicated by a coordination or abstraction of chloride as will be documented on the reactions with 2,2′-bipyridine (**bpy**), 1,10-phenanthroline (**phen**) and *trans-N*-(2-pyridylmethylene)-aniline (**pyma**).

Reaction of **2** with two equivalents of **bpy**, **phen** and **pyma** gives, after standard work up, the desired η^3-indenyl compounds $[(\eta^3\text{-}4,7\text{-}Me_2C_9H_5)Mo(CO)_2(^{N,N}L)Cl]$ (**4a**: $^{N,N}L$ = bpy, **5a**: $^{N,N}L$ = phen, **6a**: $^{N,N}L$ = pyma), see Scheme 3. Infrared spectra of the solid-state samples show two CO stretching bands at low frequencies (Table 2) indicating the proposed neutral

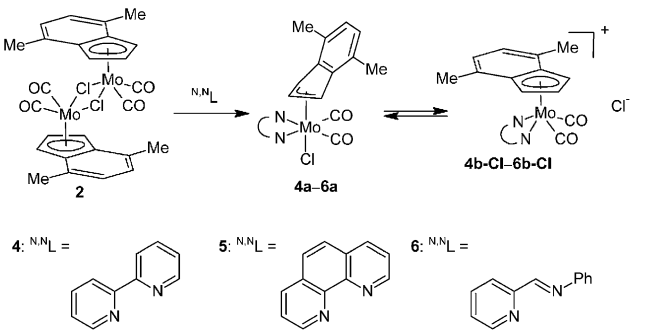

Scheme 3 Reaction of **2** with two equivalents of **bpy**, **phen** and **pyma**.

Open Access Article. Published on 16 March 2015. Downloaded on 5/9/2026 9:53:25 AM.
This article is licensed under a Creative Commons Attribution-NonCommercial 3.0 Unported Licence.

Table 1 Geometric parameters of the neutral and cationic pentacoordinated molybdenum species[a]

	3[e]	4b-BF_4	5b-9·CH_2Cl_2	8-BF_4	10b-BF_4·0.5(Me_2-phen·HBF_4)
Mo–Cg(C_5)	2.0236(9)	1.9979(12)	2.004(3)	1.990(2)	2.0154(18)
Mo–C(CO)	1.929(2)	1.960(3)	1.950(9)	1.968(5)	1.945(6)
	1.956(2)	1.970(3)	1.980(9)	1.969(4)	1.957(6)
Mo–N	2.280(2)	2.190(2)	2.196(5)	2.180(4)	2.244(4)
		2.191(2)	2.208(6)	2.182(4)	2.250(4)
C(CO)–Mo–C(CO)	72.71(10)	74.72(12)	74.8(4)	74.3(2)	69.5(2)
N–Mo–N	—	72.88(8)	73.3(2)	78.93(14)	74.45(13)
Pl^1–Pl^2[b]	—	7.8(2)	6.8(4)	—	22.4(2)
Ω[c]	7.4(2)	5.1(3)	5.7(8)	6.7(5)	6.3(4)
Δ(M–C)[d]	0.212(2)	0.149(3)	0.157(8)	0.160(5)	0.178(4)

[a] Distances are given in Å; angles and dihedral angles are given in °. [b] Pl^1 is defined by Mo and two nitrogen donor atoms; Pl^2 is defined by two nitrogen donor atoms and two adjacent carbon atoms of the chelate ring. [c] Ω is the envelope fold angle defined for the indenyl ligand as the angle between planes defined by C3, C4 and C5 and that of C1, C2, C3 and C5.[41] [d] Δ(M–C) represents the differences in the metal–carbon bonds. It is defined for the indenyl compounds as the difference between the averages of the metal–carbon distances M–C1 and M–C2 and those of M–C3, M–C4, and M–C5.[41] [e] Mo–Cl = 2.4998(6) Å; N–Mo–Cl = 82.24(4)°.

structure. Hence, cationic complexes $[(\eta^5\text{-Ind})Mo(CO)_2L_2]^+$ have much lower electron density on molybdenum atom than neutral compounds with slipped indenyl ring $[(\eta^3\text{-Ind})Mo(CO)_2L_2Cl]$ as could be documented on the CO stretching band frequencies of the pairs bearing monodentate ligands (*cf.* data for compounds bearing DMF or MeCN in Table 2).

The solid state structure of the compound **6a** was determined by X-ray diffraction analysis, see Fig. 2. The molecule has a distorted octahedral structure. When the bond Cg(C_3)–Mo is defined as the principal axis, indenyl and chloride occupy the axial positions while the *cis*-coordinated carbonyl ligands and the nitrogen donor atoms of pyma are in the equatorial plane. High values of Ω [23.1(6)°] and Δ(M–C) [0.849(6) Å], observed for indenyl ligand, are in line with desired η^3-coordination mode.[22,42,43] According to the initial aim, the compound **6a** is isostructural with allyl complex $[(\eta^3\text{-}C_3H_5)Mo(CO)_2(pyma)Cl]$ (**6-allyl**) that was also confirmed by X-ray diffraction analysis (*cf.* Fig. 2 and 3). The allyl counterpart **6-allyl** was prepared by a ligand exchange reaction starting from $[(\eta^3\text{-}C_3H_5)Mo(CO)_2(NCMe)_2Cl]$ and **pyma**. The geometric parameters of **6a** and **6-allyl**, describing the coordination sphere of molybdenum, are very similar (see Table 3). Only the distance Mo–Cg(C_3) in **6a** is longer due to an electron-withdrawing character of the annulated benzene ring that weakens the donor properties of indenyl.

Although the indenyl compounds **4a–6a** are isostructural with the well-known allyl complexes $[(\eta^3\text{-}C_3H_5)Mo(CO)_2(^{N,N}L)Cl]$ their behavior in solution is very different. The allyl compounds are stable in solution of common organic solvents while a dissolution of the η^3-indenyl compounds **4a–6a**, even in non-coordinating solvents, leads to a chloride abstraction to give cationic pentacoordinated species $[(\eta^5\text{-}4,7\text{-}Me_2C_9H_5)Mo(CO)_2(^{N,N}L)]^+$ (**4b**: $^{N,N}L$ = bpy, **5b**: $^{N,N}L$ = phen, **6b**: $^{N,N}L$ = pyma) as evidenced by the ^1H NMR spectroscopy, see Scheme 3. The complexes bearing bpy (**4a**) and phen (**5a**) undergo a complete ionization in solution while the compound **6a** only a

Table 2 Summary of the infrared data for the molybdenum complexes[a]

	ν_a(CO)	ν_s(CO)	Ref.
4a	1940	1862	
4b-BF_4	1970	1894	
$[(\eta^5\text{-Ind})Mo(CO)_2(bpy)][BF_4]$	1974	1878	13
5a	1919	1844	
5b-BF_4	1967	1880	
$[(\eta^5\text{-Ind})Mo(CO)_2(phen)][BF_4]$	1968	1874	13
6a	1934	1855	
$[(\eta^3\text{-Ind})Mo(CO)_2(NCMe)_2Cl]$	1954	1851	23
$[(\eta^5\text{-Ind})Mo(CO)_2(NCMe)_2][BF_4]$	1970	1880	23
$[(\eta^3\text{-Ind})Mo(CO)_2(DMF)_2Cl]$	1934	1830	24
$[(\eta^5\text{-Ind})Mo(CO)_2(DMF)_2][BF_4]$	1962	1865	24

[a] The stretching frequencies are given in cm^{-1}.

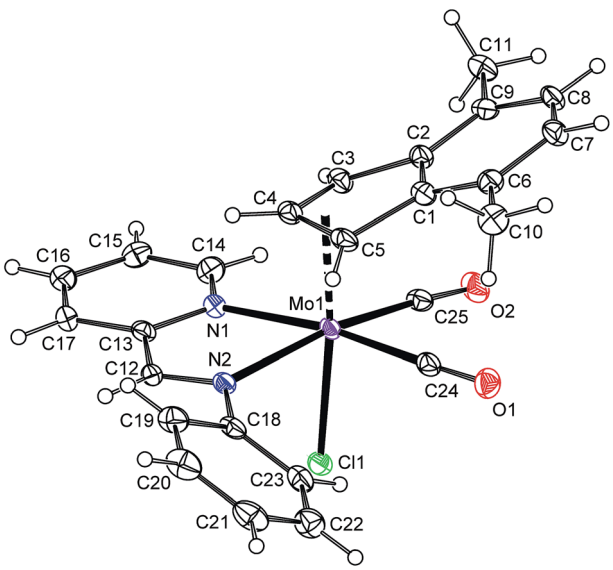

Fig. 2 ORTEP drawing of $[(\eta^3\text{-}4,7\text{-}Me_2C_9H_5)Mo(CO)_2(pyma)Cl]$ (**6a**). The labeling for all non-hydrogen atoms is shown. Thermal ellipsoids are drawn at the 30% probability level.

 This journal is © The Royal Society of Chemistry 2015

Open Access Article. Published on 16 March 2015. Downloaded on 5/9/2026 9:53:25 AM.
This article is licensed under a Creative Commons Attribution-NonCommercial 3.0 Unported Licence.

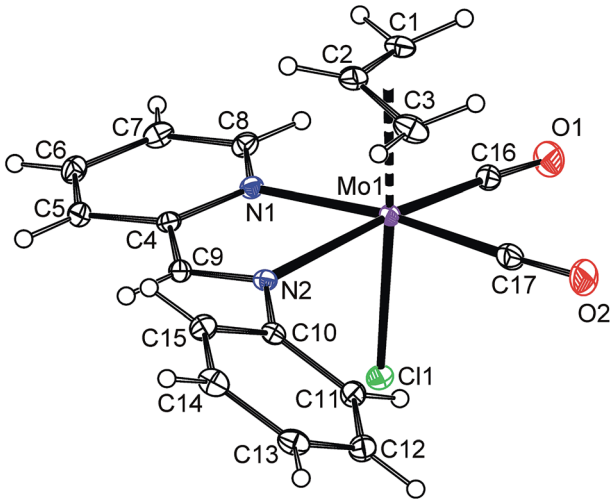

Fig. 3 ORTEP drawing of $[(\eta^3\text{-}C_3H_5)Mo(CO)_2(pyma)Cl]$ (**6-allyl**). The labeling for all non-hydrogen atoms is shown. Thermal ellipsoids are drawn at the 30% probability level.

partial one as evidenced by two sets of signals. It suggests that the chloride abstraction is an equilibrium reaction that is further supported by a fact that a solvent evaporation gives back the initial hexacoordinated species **4a–6a**, see Scheme 3.

The assignment of the sets of signals to the η^3 -or η^5-indenyl species is done according to chemical shift of the proton at the 2-position. Hence, low-fielded triplet of H^2 is diagnostic to η^3-coordination mode while high-fielded one implies the η^5-bonding of the indenyl ligand.[40] This assignment is confirmed by the use of an alternative chloride-free protocol for the cationic species **4b** and **5b** compensated with a weakly coordinating tetrafluoroborate, see Scheme 4.

Protonation of allyl compound $[(\eta^3\text{-}C_3H_5)(\eta^5\text{-}4,7\text{-}Me_2C_9H_5)Mo(CO)_2]$ (7) in presence of acetonitrile gives the cationic compound $[(\eta^5\text{-}4,7\text{-}Me_2C_9H_5)Mo(CO)_2(NCMe)_2][BF_4]$ (**8-BF$_4$**). Following ligand exchange produces the desired chelate complexes $[(\eta^5\text{-}4,7\text{-}Me_2C_9H_5)Mo(CO)_2(bpy)][BF_4]$ (**4b-BF$_4$**) and $[(\eta^5\text{-}4,7\text{-}Me_2C_9H_5)Mo(CO)_2(phen)][BF_4]$ (**5b-BF$_4$**). As expected, the solution ^1H NMR spectra are identical with chloride analogues **4b-Cl** and **5b-Cl**. High CO stretching frequencies observed for solid samples of **4b-BF$_4$** and **5b-BF$_4$** are in line with the presence of weakly coordinating anion (*cf.* with **4a** and **5a** in Table 2) and prove retention of **4b-BF$_4$** and **5b-BF$_4$** in the solid state. The structures of **8-BF$_4$** and **4b-BF$_4$** were determined by X-ray diffraction analysis. Both cations have a square-pyramidal structure, see Fig. 4 and 5. The apical position is occupied with the η^5-bonded indenyl ligand (for Ω and Δ(M–C) see Table 1). The *cis*-coordinated carbonyl ligands and two nitrogen donor atoms of remaining ligands form the basal plane. The structural parameters, describing the coordination sphere of molybdenum, are in line with data of structurally related cyclopentadienyl and indenyl compounds described previously.[13,14,44–46]

The reaction of **2** with lower than stoichiometric amount of **bpy** or **phen** gives a material insoluble in common organic solvents that strongly contrasts with properties of the starting compounds as well as the products **4a** and **5a**. Elemental analysis of the products together with their insolubility suggests an appearance of the ionic pair consisting of a large complex cation and a large complex anion $[(\eta^5\text{-}4,7\text{-}Me_2C_9H_5)Mo(CO)_2(^{N,N}L)]$ $[(\eta^5\text{-}4,7\text{-}Me_2C_9H_5)Mo(CO)_2Cl_2]$ (**4b-9:** $^{N,N}L$ = bpy, **5b-9:** $^{N,N}L$ = phen), see Scheme 5. Slow diffusion of a phenanthroline solution into a solution of the starting compound (**2**) gives single crystals suitable for the X-ray diffraction analysis that confirmed the proposed ionic structure of **5b-9** (see Fig. 6). The cationic part is isostructural with bipyridine complex **4b-BF$_4$**. The anionic part forms square-pyramid with two *cis*-coordinated carbonyl ligands and two chlorides in basal plane. The η^5-coordinated indenyl (for Ω and Δ(M–C) see Table 4) occupies the apical position. The geometric parameters describing the coordination sphere of anionic part are very close to the data recently published for starting dimeric species $[\{(\eta^5\text{-}4,7\text{-}Me_2C_9H_5)Mo(CO)_2(\mu\text{-}Cl)\}_2]$ (**2**).[22] The crystal structure of **5b-9** is stabilized by intramolecular π–π stacking involving phenanthroline ligand of **5b** and indenyl ligand of **9**. The distance between the centroid of central phenanthroline ring and centroid of the C_6-ring of the indenyl ligand was found to be 3.493(5) Å.

Since the anionic complex (**9**) is unprecedented an alternative method of the synthesis was developed. It is given by the reaction of **2** with a common source of chlorides. Namely, the soluble ammonium salt, $[Me_4N][(\eta^5\text{-}4,7\text{-}Me_2C_9H_5)Mo(CO)_2Cl_2]$ (**Me$_4$N-9**), was prepared by the reaction of **2** with $[Me_4N]Cl$ (Scheme 6). The infrared spectra of **Me$_4$N-9** show the CO stretching bands at low wavenumbers [ν_a(CO): 1936, 1922 cm^{-1}; ν_s(CO): 1820 cm^{-1}] that is consistent with the high electron density on molybdenum. The appearance of two bands of the ν_a(CO) is due to a vibration coupling of the carbonyl ligands in the crystal lattice. ^1H NMR spectrum of **Me$_4$N-9** shows a typical pattern of the η^5-indenyl ligand with a highfielded signal of H^2 (δ = 4.87 ppm).

Reaction of 2 with sterically demanding *N,N*-chelating ligands

Dissociation of the complexes bearing **bpy**, **phen** and **pyma** led us to a more sterically demanding *N,N*-chelating ligand,

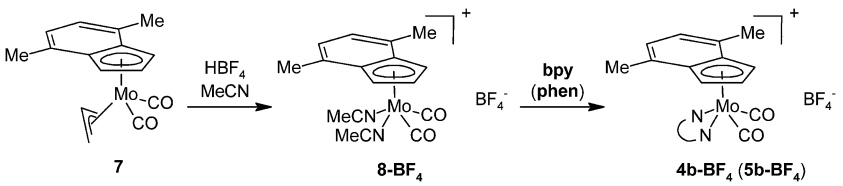

Scheme 4 Synthesis of cationic molybdenum compounds.

Open Access Article. Published on 16 March 2015. Downloaded on 5/9/2026 9:53:25 AM.
This article is licensed under a Creative Commons Attribution-NonCommercial 3.0 Unported Licence.

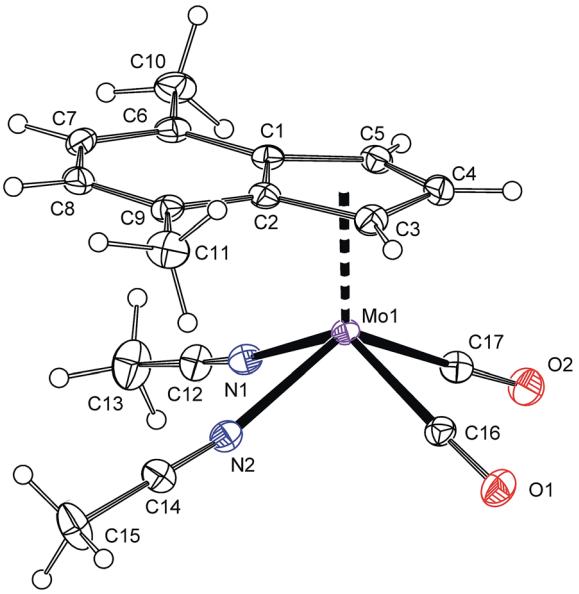

Fig. 4 ORTEP drawing of cation $[(\eta^5\text{-}4,7\text{-}Me_2C_9H_5)Mo(CO)_2(NCMe)_2]^+$ present in the crystal structure of **8-BF$_4$**. The labeling for all non-hydrogen atoms is shown. Thermal ellipsoids are drawn at the 30% probability level.

2,9-dimethyl-1,10-phenanthroline (2,9-Me_2-phen), in attempt to stabilize the η^3-indenyl species in solution.

The product of the reaction between $[\eta^5\text{-}4,7\text{-}Me_2C_9H_5)Mo(CO)_2(\mu\text{-}Cl)\}_2]$ (**2**) and 2,9-Me_2-phen shows similar frequencies of the CO stretching bands [ν_a(CO): 1927 cm^{-1}; ν_s(CO): 1848 cm^{-1}] as observed for the hexacoordinated species **4a–6a** that

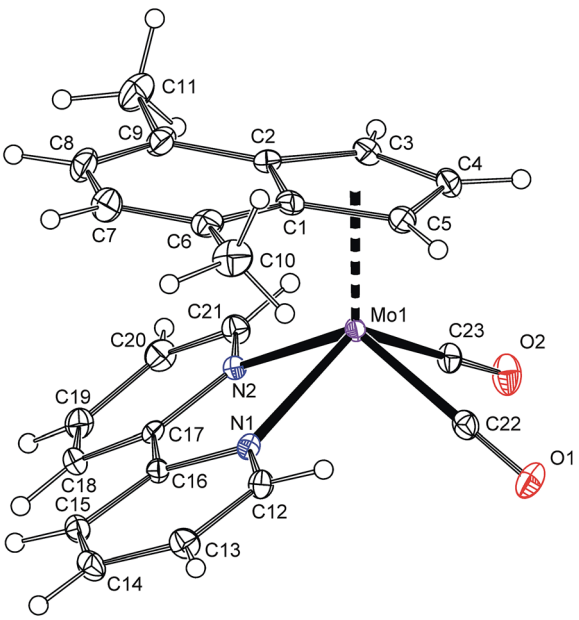

Fig. 5 ORTEP drawing of cation $[(\eta^5\text{-}4,7\text{-}Me_2C_9H_5)Mo(CO)_2(bpy)]^+$ present in the crystal structure of **4b-BF$_4$**. The labeling for all non-hydrogen atoms is shown. Thermal ellipsoids are drawn at the 30% probability level.

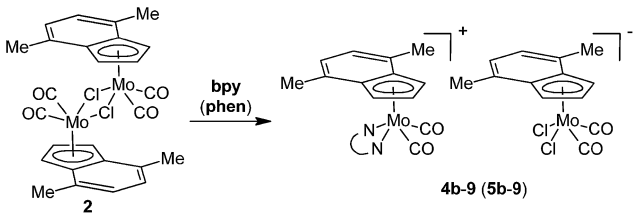

Scheme 5 Reaction of **2** with one equivalent of **bpy** or **phen**.

implies a similar molecular structure in the solid state, $[(\eta^3\text{-}4,7\text{-}Me_2C_9H_5)Mo(CO)_2(2,9\text{-}Me_2\text{-phen})Cl]$ (**10a**), see Scheme 7. The enhanced stability of **10a** in solution was confirmed by ^{1}H NMR spectroscopy. Hence, the spectrum shows only one set of signals. The signal of the indenyl proton H^2 appears at high field (δ = 5.84 ppm) that is typical for η^3-coordination mode. The observed spectrum pattern is consistent with C_s molecular symmetry that confirms a configuration with the nitrogen donor atoms of the chelating ligand in *trans*-positions to the *cis*-coordinated carbonyl ligands. The X-ray structure analyses of **10a**·CH_2Cl_2 and **10a**·$CHCl_3$ confirm appearance of this isomer in the solid state, see Fig. 7. The η^3-coordination mode of the indenyl ligand is evidenced by slipping parameters Ω (~23°) and Δ(M–C) (~0.84 Å), see Table 3.

Although the coordination sphere of molybdenum seems to be very similar to the pyma complex **6a** (*cf.* bond distances and bond angles in Table 3), the methyl groups in the near neighborhood of carbonyl ligands prevent an appearance of a planar chelate cycle. Hence, the methyl groups of 2,9-Me_2-phen are forced below the equatorial plane, defined by molybdenum and carbonyl ligands, that causes an envelope folding of the chelate cycle of ~14°. This distortion is caused by steric repulsion of the

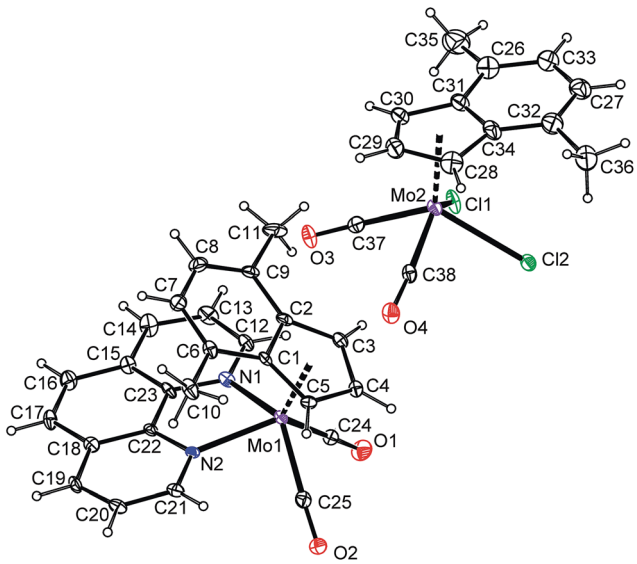

Fig. 6 ORTEP drawing of $[(\eta^5\text{-}4,7\text{-}Me_2C_9H_5)Mo(CO)_2(bpy)]^+$ and $[(\eta^5\text{-}4,7\text{-}Me_2C_9H_5)Mo(CO)_2Cl_2]^-$ present in the crystal structure of **5b-9**·CH_2Cl_2. The labeling for all non-hydrogen atoms is shown. Thermal ellipsoids are drawn at the 20% probability level.

This journal is © The Royal Society of Chemistry 2015

Open Access Article. Published on 16 March 2015. Downloaded on 5/9/2026 9:53:25 AM.
This article is licensed under a Creative Commons Attribution-NonCommercial 3.0 Unported Licence.

Table 3 Geometric parameters of the neutral hexacoordinated molybdenum species[a]

	6a	6-allyl	10a·CH_2Cl_2[b]	10a·CH_2Cl_2[b]	10a·$CHCl_3$	10-allyl	10c
Mo–Cg(C_3)	2.1027(18)	2.040(2)	2.106(3)	2.109(2)	2.1202(16)	2.040(5)	2.126(3)
Mo–X	2.4736(14)	2.4957(5)	2.4649(7)	2.4761(7)	2.4690(7)	2.4858(4)	2.6189(4)
Mo–C(CO)	1.977(7)	1.957(3)	1.957(2)	1.953(2)	1.945(3)	1.9466(14)	1.958(3)
	1.964(5)	1.959(3)	1.958(2)	1.957(2)	1.966(2)	1.9498(15)	1.960(3)
Mo–N	2.231(6)	2.248(2)	2.277(2)	2.279(2)	2.280(2)	2.2984(11)	2.261(2)
	2.262(4)	2.279(2)	2.283(2)	2.281(2)	2.287(2)	2.2958(11)	2.283(2)
Cg(C_3)–Mo–X	173.35(8)	175.83(9)	174.81(7)	175.27(6)	176.05(6)	177.20(6)	175.49(8)
C(CO)–Mo–C(CO)	79.1(3)	78.02(11)	76.15(10)	77.30(10)	75.27(12)	76.75(6)	75.07(12)
N–Mo–N	73.25(18)	72.39(7)	74.26(6)	73.85(7)	73.59(7)	73.06(4)	74.57(9)
Pl^1–Pl^2[c]	2.0(3)	0.4(1)	10.0(2)	14.4(2)	13.2(2)	14.11(8)	9.8(2)
Ω[c]	23.1(6)	—	23.2(3)	23.4(2)	22.5(3)	—	21.3(3)
Δ(M–C)[c]	0.849(6)	—	0.840(3)	0.847(3)	0.838(3)	—	0.805(3)

[a] Distances are given in Å; angles and dihedral angles are given in °. [b] Two crystallographically independent molecules in the unit cell. [c] For definition see footnote of Table 1.

methyl groups with the carbonyl ligands as evidenced by short nonbonding distances C(CH_3)–C(CO) of 3.064(4)–3.138(4) Å those are considerably shorter than sum of van der Waals radii of two carbon atoms (3.4 Å).[47] The folding of the chelate cycle seems to be independent on nature of η^3-ligands. Hence, the η^3-allyl analogue **10-allyl** is distorted in the same way as **10a**; *cf.* Fig. 7 and 8 and Pl_1–Pl_2 in Table 3.

The high stability of **10a** toward the loss of chloride suggests that the cationic complex bearing 2,9-Me_2-phen, **10b-BF$_4$**, should be a suitable precursor for the assembly of hexacoordinated complexes bearing various anionic 2e ligands (Scheme 8). The starting **10b-BF$_4$** was synthesized using the standard protocol outlined above for **4b-BF$_4$**. The X-ray diffraction analysis of the **10b-BF$_4$**·0.5(Me_2-phen·HBF_4) reveals the expected square-pyramidal structure (Fig. 9) with the η^5-coordinated indenyl ligand as documented by slippage parameters [Ω = 6.3(4)°; Δ(M–C) [0.178(4) Å]. The folding of the chelate cycle [Pl_1–Pl_2 is 22.4(2)°] is, in this case, much heavier than observed for 2,2′-bipyridine analogue **4b-BF$_4$** [7.8(2)°] and even that in hexacoordiated species **10a** [10.0(2)–14.4(2)°]. This distortion is

Table 4 Geometric parameters of the anionic molybdenum species [(η^5-4,7-$Me_2C_9H_5$)Mo(CO)$_2$$Cl_2$]$^-$ present in the crystal structure of **5b-9**·CH_2Cl_2[a]

Mo–Cg(C_5)	2.036(4)	C(CO)–Mo–C(CO)	74.0(4)
Mo–C(CO)	1.942(9)	Cl–Mo–Cl	81.56(8)
	1.909(9)		
Mo–Cl	2.495(2)	Ω[b]	9.9(10)
	2.514(2)		
		Δ(M–C)[b]	0.239(10)

[a] Distances are given in Å, angles and dihedral angles are given in °. [b] For definition see footnote of Table 1.

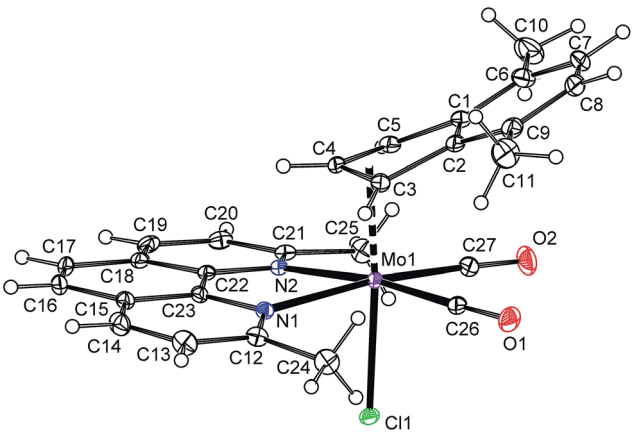

Fig. 7 ORTEP drawing of [(η^3-4,7-$Me_2C_9H_5$)Mo(CO)$_2$(2,9-Me_2-phen)Cl] present in the crystal structure of **10a**·CH_2Cl_2. The labeling for all non-hydrogen atoms is shown. Thermal ellipsoids are drawn at the 30% probability level. Only one of two crystallographically independent molecules is shown for clarity.

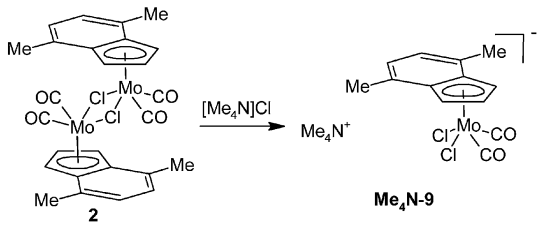

Scheme 6 Synthesis of [Me_4N][(η^5-4,7-$Me_2C_9H_5$)Mo(CO)$_2$$Cl_2$] (**Me$_4$N-9**).

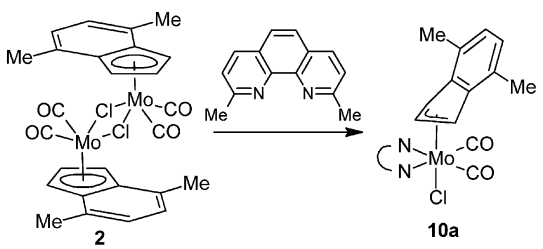

Scheme 7 Synthesis of [(η^3-4,7-$Me_2C_9H_5$)Mo(CO)$_2$(2,9-Me_2-phen)Cl] (**10a**).

Open Access Article. Published on 16 March 2015. Downloaded on 5/9/2026 9:53:25 AM.
This article is licensed under a Creative Commons Attribution-NonCommercial 3.0 Unported Licence.

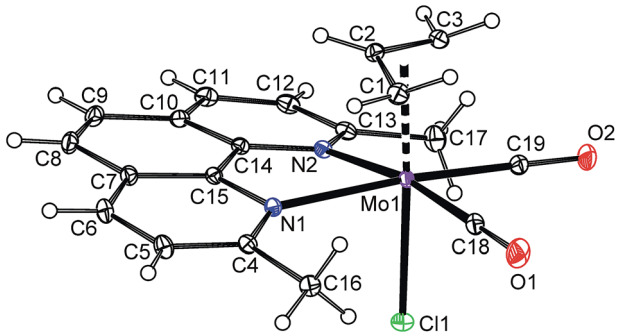

Fig. 8 ORTEP drawing of $[(\eta^3\text{-}C_3H_5)Mo(CO)_2(2,9\text{-}Me_2\text{-}phen)Cl]$ (**10-allyl**). The labeling for all non-hydrogen atoms is shown. Thermal ellipsoids are drawn at the 30% probability level.

accompanied with prolongation of the bonds Mo–N (*cf.* **10b-BF$_4$**·0.5(Me_2-phen·HBF_4) with **4b-BF$_4$** and **5b-9**·CH_2Cl_2 in Table 1). These observations imply that a repulsion of the phenanthroline methyl groups from the carbonyl ligands is weaker for hexacoordinated species and seems to be a driving force for its stabilization in solution. The crystal structure of **10b-BF$_4$**·0.5(Me_2-phen·HBF_4) reveals π–π stacking interactions involving two molecules of cationic complex **10b** and a protonated ligand. The distance between centroid of the central phenanthroline rings are 3.598(3) Å.[48]

The instability of the pentacoordinated cationic species in presence of free monoanionic ligands was evidenced on reactions of **10b-BF$_4$** with a series of halides and pseudohalides. An apearance of the hexacoordinated species $[(\eta^3\text{-}4,7\text{-}Me_2C_9H_5)Mo(CO)_2(2,9\text{-}Me_2\text{-}phen)X]$ (**10a:** X = Cl, **10c:** X = Br, **10d:** X = I, **10e:** X = NCO, **10f:** X = NCS) is documented by the infrared and NMR spectroscopy. The compounds **10c–10f** are stable in solution. The ^{1}H NMR spectra of the isolated products confirm that the dissociation reaction is highly disfavored similarly as in case of the parent chloride complex **10a.** The infrared spectra reveal that cyanate ligand in **10e** and thiocyanate ligand in **10f** are bonded to molybdenum *via* the nitrogen donor atom. It is documented by low stretching frequencies of the C=N bonds (**10e:** 2195 cm^{-1}, **10f:** 2063 cm^{-1}). This observation is in line with literature data reported for allyl analogues $[(\eta^3\text{-}C_3H_5)Mo(CO)_2(Ph_2PCH_2CH_2PPh_2)(NCO)]$,[49] $[(\eta^3\text{-}C_3H_5)Mo(CO)_2(phen)(NCS)]$,[50,51] $[(\eta^3\text{-}C_3H_4Ph)Mo(CO)_2(phen)(NCS)]$,[52] $[(\eta^3\text{-}C_3H_5)Mo(CO)_2(NCMe)_2(NCS)]$.[53] Structure of the bromide complex **10c** was determined by X-ray analysis, see Fig. 10. The coordination sphere of the central metal is very similar as in case of the chloride

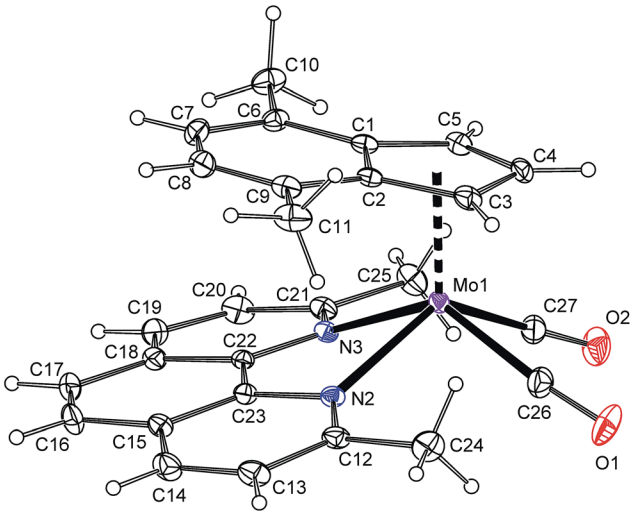

Fig. 9 ORTEP drawing of cation $[(\eta^5\text{-}4,7\text{-}Me_2C_9H_5)Mo(CO)_2(2,9\text{-}Me_2\text{-}phen)]^+$ present in the crystal structure of **10b-BF$_4$**·0.5(Me_2-phen·HBF_4). The labeling for all non-hydrogen atoms is shown. Thermal ellipsoids are drawn at the 20% probability level.

analogue **10a.** The bond distance Mo–Br was found to be shorter [2.6189(4) Å] than in case of similar allyl complexes $[(\eta^3\text{-}C_3H_5)Mo(CO)_2(^{N,N}L)Br]$ (^{N,N}L = bpy: 2.650(3) Å, ^{N,N}L = phen: 2.645(2) Å] that is a result of different donor properties of the ligand in *trans*-possition to bromide.[54]

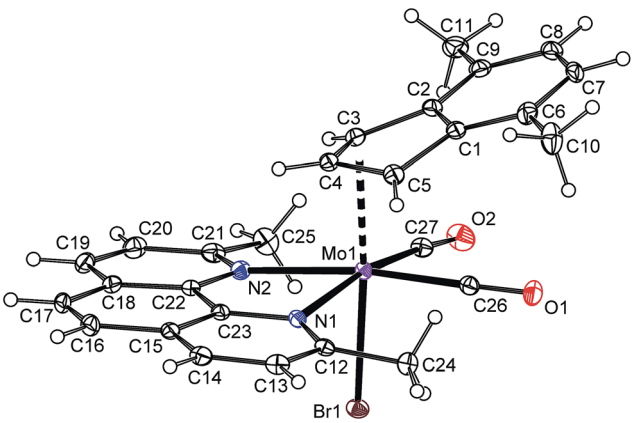

Fig. 10 ORTEP drawing of $[(\eta^3\text{-}4,7\text{-}Me_2C_9H_5)Mo(CO)_2(2,9\text{-}Me_2\text{-}phen)Br]$ present in the crystal structure of **10c**. The labeling for all non-hydrogen atoms is shown. Thermal ellipsoids are drawn at the 30% probability level.

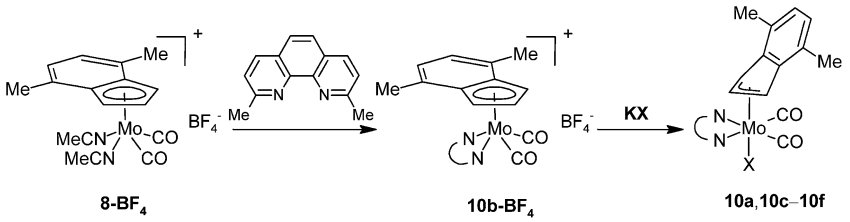

Scheme 8 Optimized synthesis of η^3-indenyl compounds. X = Cl, Br, I, NCO and NCS for compounds denoted **a**, **c**, **d**, **e** and **f**, respectively.

This journal is © The Royal Society of Chemistry 2015

Open Access Article. Published on 16 March 2015. Downloaded on 5/9/2026 9:53:25 AM.
This article is licensed under a Creative Commons Attribution-NonCommercial 3.0 Unported Licence.

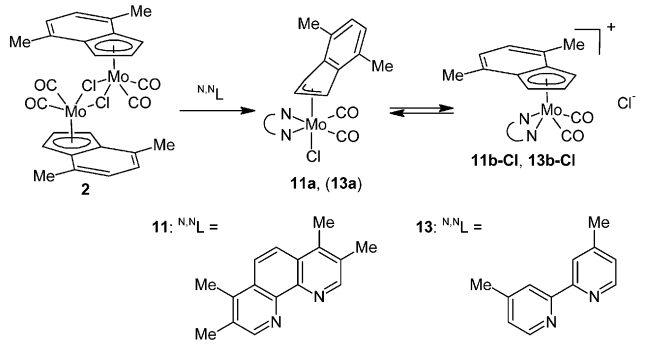

Scheme 9 Reaction of **2** with two equivalents of 3,4,7,8-Me_4-phen and 4,4′-Me_2-bpy.

A variation of the electronic properties of the bidentate ligands has only minor effect on stability of the η^3-indenyl complexes as documented on experiments with series of modified *N,N*-chelating ligands, namely 3,4,7,8-Me_4-phen, 2,9-Me_2-4,7-Ph_2-phen, 4,4′-Me_2-bpy and 6,6′-Me_2-bpy. Although the donor ability of the 1,10-phenanthroline ligands decreases in the line 3,4,7,8-Me_4-phen > 2,9-Me_2-4,7-Ph_2-phen > 2,9-Me_2-phen > phen,[55,56] the stability of the molybdenum complexes does not follow this relation. Derivatives bearing methyl groups beside the nitrogen donor atom (*i.e.* 2,9-Me_2-phen and 2,9-Me_2-4,7-Ph_2-phen) form much more stable complexes (**10a** and **12a**) than the rest of the series (*i.e.* phen and 3,4,7,8-Me_4-phen), see Schemes 3, 9 and 10. Hence, complexes **10a** and **12a** are stable in solution, while compounds **5a** and **11a** undergo dissociation giving cationic complexes **5b-Cl** and **11b-Cl**, respectively. These observations reveal that the stability of the products is mainly influenced by steric effects of the chelating ligands, overshadowing the electronic ones. Similar conclusion was achieved based on experiments with dimethyl substituted 2,2′-bipyridines. Although donor ability of 4,4′-Me_2-bpy is comparable to 6,6′-Me_2-bpy, only the later ligand gives a stable hexacoordinated species (**14a**) that does not undergo dissociation in solution and cloud be easily synthesized by reaction of **14b-BF_4** with common source of chlorides (*e.g.* $[Me_4N]Cl$), see Scheme 10. In contrary, 4,4′-Me_2-bpy produces complex with ionic structure (**13b-Cl**) both in solution and in solid state, see Scheme 9.

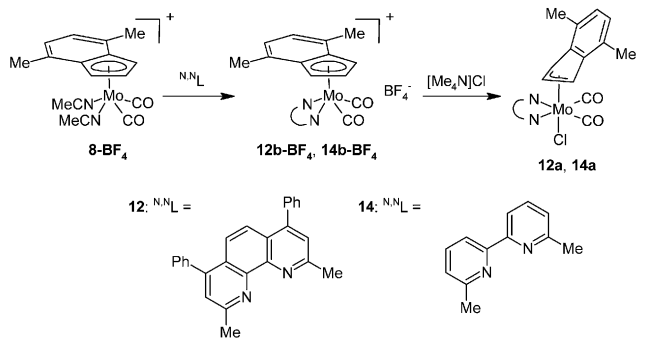

Scheme 10 Syntheses of complexes bearing 2,9-Me_2-4,7-Ph_2-phen and 6,6′-Me_2-bpy.

Conclusions

Although sterically demanding ligands are commonly used for the stabilization of low-coordinate metal compounds[57,58] or complexes in a low oxidation state,[59,60] an application of this approach for the stabilization of low hapticity of the indenyl ligand is rather unusual.[25] In current study, we clearly demonstrated that modification of the steric properties of a *N,N*-chelating ligand is a suitable approach for the hapticity adjustment in the indenyl molybdenum compounds. Hence, powerful steric effect of methyl groups in positions beside nitrogen donor atoms activates $[(\eta^5\text{-}4,7\text{-}Me_2C_9H_5)Mo(CO)_2]^+$ core toward association of 2e anionic ligand (*e.g.* halide) that is otherwise highly disfavored. Such nucleophile-induced indenyl ring slippage enables the assembly of η^3-indenyl species isostructural with highly attended allyl complexes. This observation strongly contrasts with less demanding ligands (*e.g.* bpy, 4,4′-Me_2-bpy, phen, 3,4,7,8-Me_4-phen) those form penta-coordinated cationic species $[(\eta^5\text{-}4,7\text{-}Me_2C_9H_5)Mo(CO)_2(^{N,N}L)]^+$ in solution and desired η^3-compounds were stable only in particular cases in the solid state.

Experimental section

Methods and materials

All operations were performed under nitrogen using conventional Schlenk-line techniques. The solvents were purified and dried by standard methods.[61] Starting materials were available commercially or prepared according to literature procedures: $[\{(\eta^5\text{-}4,7\text{-}Me_2C_9H_5)Mo(CO)_2(\mu\text{-}Cl)\}_2]$ (**2**),[22] $[(\eta^3\text{-}C_3H_5)(\eta^5\text{-}4,7\text{-}Me_2C_9H_5)Mo(CO)_2]$ (**7**),[22] $[(\eta^3\text{-}C_3H_5)Mo(CO)_2(NCMe)_2Cl]$,[62] The infrared spectra were recorded in the 4000−400 cm^{-1} region (resolution 2 cm^{-1}) on a Nicolet Magna 6700 FTIR spectrometer using a Diamond Smart Orbit ATR. ^1H and $^{13}C\{^1H\}$ NMR spectra were measured on a Bruker Avance 400 and a Bruker Avance 500 spectrometers at room temperature. The chemical shifts are given in ppm relative to TMS.

Synthesis of 6,6′-dimethyl-2,2′-bipyridine (6,6′-Me_2-bpy)

A solution of **bpy** (1.00 g, 6.4 mmol) in THF (100 mL) was cooled at −50 °C, treated with MeLi (17 mL, 1.6 mol L^{-1}, 27.2 mmol) and stirred at this temperature for 1 h. The solution was warmed to room temperature, stirred for another 1 h and then refluxed overnight. After cooling at room temperature, the reaction mixture was transferred into a mixture ice-water. The organic layer was separated and the aqueous layer was extracted three times with CH_2Cl_2. The combined organic layers were drier with $MgSO_4$ and filtered. The volatiles were vacuum evaporated on a rotavapor. Resulting brown oil was oxidized by a saturated solution of $KMnO_4$ in acetone until formation of MnO_2 ceased. The MnO_2 was removed by vacuum filtration through short pad of celite on a glass frit. Acetone was vacuum evaporated on a rotavapor and the crude product was purified by column chromatography on silica (hexane/ethyl acetate =

Open Access Article. Published on 16 March 2015. Downloaded on 5/9/2026 9:53:25 AM. This article is licensed under a Creative Commons Attribution-NonCommercial 3.0 Unported Licence.

1 : 1). R_f(TLC) = 0.70 (hexane/ethyl acetate = 1 : 1). Yield: 0.29 g (25%, 1.57 mmol). Analytical and spectroscopic date were consistent with those reported elsewhere.[63]

Synthesis of [(η^5-4,7-$Me_2C_9H_5$)Mo(CO)$_2$(py)Cl] (3)

[{(η^5-4,7-$Me_2C_9H_5$)Mo(CO)$_2$(μ-Cl)}$_2$] (**2**; 200 mg, 0.30 mmol) was dissolved in CH_2Cl_2 (50 mL) and treated with **py** (475 mg, 6.0 mmol). The solution was stirred at room temperature overnight. The volatiles were vacuum evaporated. The crude product was washed with ether and recrystallized from the mixture CH_2Cl_2/ether and vacuum dried. Yield: 205 mg (83%, 0.50 mmol). Red powder. Mp: 150–160 °C (dec.). Anal. calcd for $C_{18}H_{16}ClMoNO_2$: C, 52.77; H, 3.94; N, 3.42. Found: C, 52.98; H, 3.87; N, 3.60. ^{1}H NMR ($CDCl_3$; 400 MHz; δ (ppm)): 8.70 (s-br, 1H, py), 8.13 (dd, $^3J(^1H,^1H)$ = 6.4 Hz, $^4J(^1H,^1H)$ = 1.4 Hz, 2H, py), 7.68 (tt, $^3J(^1H,^1H)$ = 7.6 Hz, $^4J(^1H,^1H)$ = 1.4 Hz, 1H, py), 7.11 (m, 1H, py), 7.03 (d, $^3J(^1H,^1H)$ = 7.2 Hz, 1H, C_9H_5, $H^{5,6}$), 6.91 (d, $^3J(^1H,^1H)$ = 7.2 Hz, 1H, C_9H_5, $H^{5,6}$), 5.87 (d, $^3J(^1H,^1H)$ = 2.8 Hz, $^4J(^1H,^1H)$ = 1.5 Hz, 1H, C_9H_5, $H^{1,3}$), 5.69 (d, $^3J(^1H,^1H)$ = 2.8 Hz, $^4J(^1H,^1H)$ = 1.5 Hz, 1H, C_9H_5, $H^{1,3}$), 5.31 (t, $^3J(^1H,^1H)$ = 2.8 Hz, 1H, C_9H_5, H^2), 2.37 (s, 3H, CH_3), 1.47 (s, 3H, CH_3). FTIR (ATR, cm^{-1}): 1940 vs [ν_{sa}(CO)], 1848 vs [ν_s(CO)], 1819 vs [ν_s(CO)]. Single crystals of **3** suitable for X-ray diffraction analysis were prepared by overlayering of the CH_2Cl_2 solution with hexane.

Synthesis of [(η^3-4,7-$Me_2C_9H_5$)Mo(CO)$_2$(bpy)Cl] (4a)

[{(η^5-4,7-$Me_2C_9H_5$)Mo(CO)$_2$(μ-Cl)}$_2$] (**2**; 200 mg, 0.30 mmol) was dissolved in CH_2Cl_2 (50 mL) and treated with **bpy** (94 mg, 0.60 mmol). The solution was stirred at room temperature overnight. The volatiles were vacuum evaporated. The crude product was washed with ether and recrystallized from the mixture CH_2Cl_2/ether and vacuum dried. Yield: 285 mg (98%, 0.59 mmol). Dark red powder. Mp: 150–160 °C (dec.). Anal. calcd for $C_{23}H_{19}ClMoN_2O_2$: C, 56.75; H, 3.93; N, 5.75. Found: C, 56.92; H, 4.12; N, 5.57. ^{1}H NMR ($CDCl_3$; 400 MHz; δ (ppm); **4b-Cl**): 9.54 (s-br, 2H, bpy), 8.91 (d, $^3J(^1H,^1H)$ = 5.5 Hz, 2H, bpy), 8.22 (s-br, 2H, bpy), 7.47 (t, $^3J(^1H,^1H)$ = 6.1 Hz, 2H, bpy), 6.57 (s, 2H, C_9H_5, $H^{5,6}$), 6.09 (d, $^3J(^1H,^1H)$ = 2.6 Hz, 2H, C_9H_5, $H^{1,3}$), 5.53 (t, $^3J(^1H,^1H)$ = 2.6 Hz, 1H, C_9H_5, H^2), 1.91 (s, 6H, CH_3). FTIR (ATR, cm^{-1}): 1940 vs [ν_a(CO)], 1862 vs [ν_s(CO)].

Synthesis of [(η^5-4,7-$Me_2C_9H_5$)Mo(CO)$_2$(bpy)][BF_4] (4b-BF_4)

[(η^5-4,7-$Me_2C_9H_5$)Mo(CO)$_2$(NCMe)$_2$][BF_4] (**8-BF_4**; 100 mg, 0.22 mmol) was dissolved in CH_2Cl_2 (50 mL) and treated with **bpy** (34 mg, 0.22 mmol). The solution was stirred at room temperature overnight. The volatiles were vacuum evaporated. The crude product was washed with ether and recrystallized from the mixture CH_2Cl_2/ether and vacuum dried. Yield: 115 mg (99%, 0.21 mmol). Red powder. Mp: 180–190 °C (dec.). Anal. calcd for $C_{23}H_{19}BF_4MoN_2O_2$: C, 51.33; H, 3.56; N, 5.21. Found: C, 51.06; H, 3.71; N, 5.18. ^{1}H NMR ($CDCl_3$; 400 MHz; δ (ppm)): 8.89 (d, $^3J(^1H,^1H)$ = 5.7 Hz, 2H, bpy), 8.64 (d, $^3J(^1H,^1H)$ = 8.6 Hz, 2H, bpy), 8.14 (t, $^3J(^1H,^1H)$ = 7.8 Hz, 2H, bpy), 7.50 (t, $^3J(^1H,^1H)$ = 6.5 Hz, 2H, bpy), 6.62 (s, 2H, C_9H_5, $H^{5,6}$), 6.09 (d, $^3J(^1H,^1H)$ = 2.9 Hz, 2H, C_9H_5, $H^{1,3}$), 5.56 (t, $^3J(^1H,^1H)$ = 2.9 Hz, 1H, C_9H_5, H^2), 1.91 (s, 6H, CH_3). FTIR (ATR, cm^{-1}): 1970 vs [ν_a(CO)], 1894 vs [ν_s(CO)], 1040 vs [ν(BF)]. Single crystals of **4b-BF_4** suitable for X-ray diffraction analysis were prepared by overlayering of the CH_2Cl_2 solution with ether.

Synthesis of [(η^3-4,7-$Me_2C_9H_5$)Mo(CO)$_2$(phen)Cl] (5a)

Steps of the synthesis followed the procedure for the compounds **4a**. Reagents: [{(η^5-4,7-$Me_2C_9H_5$)Mo(CO)$_2$(μ-Cl)}$_2$] (**2**; 200 mg, 0.30 mmol) and **phen** (108 mg, 0.60 mmol). Yield: 265 mg (86%, 0.52 mmol). Dark red powder. Mp: 150–160 °C (dec.). Anal. calcd for $C_{25}H_{19}ClMoN_2O_2$: C, 58.78; H, 3.75; N, 5.48. Found: C, 58.83; H, 3.96; N, 5.44. ^{1}H NMR (CD_3CN; 400 MHz; δ (ppm); **5b-Cl**): 9.57 (dd, $^3J(^1H,^1H)$ = 5.4 Hz, $^4J(^1H,^1H)$ = 1.3 Hz, 2H, phen), 8.67 (dd, $^3J(^1H,^1H)$ = 8.3 Hz, $^4J(^1H,^1H)$ = 1.2 Hz, 2H, phen), 8.08 (s, 2H, phen), 7.94 (dd, $^3J(^1H,^1H)$ = 8.2 Hz, $^4J(^1H,^1H)$ = 5.2 Hz, 2H, phen), 6.45 (d, $^3J(^1H,^1H)$ = 2.8 Hz, 2H, C_9H_5, $H^{1,3}$), 6.16 (s, 2H, C_9H_5, $H^{5,6}$), 5.69 (t, $^3J(^1H,^1H)$ = 2.8 Hz, 1H, C_9H_5, H^2), 1.84 (s, 6H, CH_3). FTIR (ATR, cm^{-1}): 1919 vs [ν_a(CO)], 1844 vs [ν_s(CO)].

Synthesis of [(η^5-4,7-$Me_2C_9H_5$)Mo(CO)$_2$(phen)][BF_4] (5b-BF_4)

Steps of the synthesis followed the procedure for the compounds **4b-BF_4**. Reagents: [(η^5-4,7-$Me_2C_9H_5$)Mo(CO)$_2$(NCMe)$_2$][BF_4] (**8-BF_4**; 50 mg, 0.11 mmol) and **phen** (20 mg, 0.11 mmol). Yield: 65 mg (99%, 0.11 mmol). Red powder. Mp: 160–170 °C (dec.). Anal. calcd for $C_{25}H_{19}BF_4MoN_2O_2$: C, 57.08; H, 3.14; N, 4.59. Found: C, 57.17; H, 3.19; N, 4.42. ^{1}H NMR (CD_2Cl_2; 400 MHz; δ (ppm)): 9.41 (dd, $^3J(^1H,^1H)$ = 5.4 Hz, $^4J(^1H,^1H)$ = 1.2 Hz, 2H, phen), 8.62 (dd, $^3J(^1H,^1H)$ = 8.1 Hz, $^4J(^1H,^1H)$ = 1.2 Hz, 2H, phen), 8.07 (s, 2H, phen), 7.96 (dd, $^3J(^1H,^1H)$ = 8.1 Hz, $^3J(^1H,^1H)$ = 5.4 Hz, 2H, phen), 6.27 (s, 2H, C_9H_5, $H^{5,6}$), 6.27 (d, $^3J(^1H,^1H)$ = 2.8 Hz, 2H, C_9H_5, $H^{1,3}$), 5.67 (t, $^3J(^1H,^1H)$ = 2.8 Hz, 1H, C_9H_5, H^2), 1.86 (s, 6H, CH_3). ^{13}C NMR (CD_2Cl_2; 101 MHz; δ (ppm)): 252.3 (2C, *C*O), 133.1, 132.3 (2 × 1C_q), 156.6, 139.0, 129.0, 128.1, 125.1 (5 × 2C, phen and C_9H_5), 91.3 (1C, C^2 of C_9H_5), 79.5 (2C, $C^{1,3}$ of C_9H_5), 19.0 (2C, CH_3). FTIR (ATR, cm^{-1}): 1967 vs [ν_a(CO)], 1880 vs [ν_s(CO)].

Synthesis of [(η^3-4,7-$Me_2C_9H_5$)Mo(CO)$_2$(pyma)Cl] (6a)

Steps of the synthesis followed the procedure for the compounds **4a**. Reagents: [{(η^5-4,7-$Me_2C_9H_5$)Mo(CO)$_2$(μ-Cl)}$_2$] (**2**; 200 mg, 0.30 mmol) and **pyma** (109 mg, 0.60 mmol). Yield: 285 mg (93%, 0.56 mmol). Purple powder. Mp: 150–160 °C (dec.). Anal. calcd for $C_{25}H_{21}ClMoN_2O_2$: C, 58.55; H, 4.13; N, 5.46. Found: C, 58.44; H, 4.25; N, 5.59. ^{1}H NMR (CD_3CN; 400 MHz; δ (ppm); **6a** and **6b-Cl** in the ratio 1 : 3): 8.61 (d, $^3J(^1H,^1H)$ = 5.4 Hz, 1H of **a**, pyma), 8.60 (s, 1H of **a**, pyma), 8.41 (s, 1H of **b**, pyma), 8.25 (d, $^3J(^1H,^1H)$ = 7.8 Hz, 1H of **b**, pyma), 8.10 (m, 1H of **a** and 1H of **b**, pyma), 7.60–7.25 (m, 7H of **a** and 7H of **b**, pyma), 7.20 (d, $^3J(^1H,^1H)$ = 7.2 Hz, 1H of **b**, C_9H_5, $H^{5,6}$), 7.07 (d, $^3J(^1H,^1H)$ = 7.0 Hz, 1H of **a**, C_9H_5, $H^{5,6}$), 6.93 (d, $^3J(^1H,^1H)$ = 7.2 Hz, 1H of **b**, C_9H_5, $H^{5,6}$), 6.64 (d, $^3J(^1H,^1H)$ = 7.0 Hz, 1H of **a**, C_9H_5, $H^{5,6}$), 6.61 (t, $^3J(^1H,^1H)$ = 3.6 Hz, 1H of **a**, C_9H_5, H^2), 6.16 (dd, $^3J(^1H,^1H)$ = 2.8 Hz, $^4J(^1H,^1H)$ = 1.5 Hz, 1H **b**, C_9H_5, $H^{1,3}$), 6.10 (dd, $^3J(^1H,^1H)$ = 2.8 Hz, $^4J(^1H,^1H)$ = 1.5 Hz, 1H of **b**, C_9H_5, $H^{1,3}$), 5.72 (t, $^3J(^1H,^1H)$ = 2.8 Hz, 1H of **b**, C_9H_5, H^2), 5.09 (dd, $^3J(^1H,^1H)$ = 3.6 Hz, $^4J(^1H,^1H)$ = 2.5 Hz, 1H of **a**, C_9H_5, $H^{1,3}$), 4.25 (dd, $^3J(^1H,^1H)$ = 3.6 Hz, $^4J(^1H,^1H)$ = 2.5 Hz, 1H of **a**, C_9H_5, $H^{1,3}$), 2.07 (s, 3H of **a**, CH_3), 2.06 (s, 3H of **b**, CH_3),

 This journal is © The Royal Society of Chemistry 2015

Open Access Article. Published on 16 March 2015. Downloaded on 5/9/2026 9:53:25 AM.
This article is licensed under a Creative Commons Attribution-NonCommercial 3.0 Unported Licence.

1.73 (s, 3H of **a**, CH_3), 1.57 (s, 3H of **b**, CH_3). FTIR (ATR, cm^{-1}): 1934 vs [ν_a(CO)], 1855 vs [ν_s(CO)]. Single crystals of **6a** suitable for X-ray diffraction analysis were prepared by overlayering of the $CHCl_3$ solution with hexane.

Synthesis of [(η^3-C_3H_5)Mo(CO)$_2$(pyma)Cl] (6-allyl)

[(η^3-C_3H_5)Mo(CO)$_2$(NCMe)$_2$Cl] (200 mg, 0.64 mmol) was dissolved in CH_2Cl_2 (50 mL) and treated with **pyma** (117 mg, 0.64 mmol). The solution was stirred at room temperature overnight. The volatiles were vacuum evaporated. The crude product was washed with ether and recrystallized from the mixture CH_2Cl_2/ether and vacuum dried. Yield: 250 mg (95%, 0.61 mmol). Dark puple powder. Mp: 160–170 °C (dec.). Anal. calcd for $C_{17}H_{15}ClMoN_2O_2$: C, 49.72; H, 3.68; N, 6.82. Found: C, 49.61; H, 3.70; N, 6.94. ^{1}H NMR (CD_3CN; 400 MHz; δ (ppm): 8.84 (d, $^3J(^1H,^1H)$ = 5.1 Hz, 1H, pyma), 8.53 (s, 1H, pyma), 8.10 (td, $^3J(^1H,^1H)$ = 7.8 Hz, $^4J(^1H,^1H)$ = 1.4 Hz 1H, pyma), 7.98 (d, $^3J(^1H,^1H)$ = 7.6 Hz, 1H, pyma), 7.65–7.40 (m, 6H, pyma), 3.36 (tt, $^3J(^1H,^1H)$ = 9.2 Hz, $^3J(^1H,^1H)$ = 6.2 Hz, 1H, *meso*-C_3H_5), 3.16 (dd, $^3J(^1H,^1H)$ = 6.2 Hz, $^4J(^1H,^1H)$ = 3.3 Hz, 1H, *syn*-C_3H_5), 2.48 (dd, $^3J(^1H,^1H)$ = 6.2 Hz, $^4J(^1H,^1H)$ = 3.3 Hz, 1H, *syn*-C_3H_5), 1.31 (d, $^3J(^1H,^1H)$ = 9.2 Hz, 1H, *anti*-C_3H_5), 1.02 (d, $^3J(^1H,^1H)$ = 9.2 Hz, 1H, *anti*-C_3H_5). FTIR (ATR, cm^{-1}): 1929 vs [ν_a(CO)], 1845 vs [ν_s(CO)]. Single crystals of **6-allyl** suitable for X-ray diffraction analysis were prepared by overlayering of the CH_2Cl_2 solution with hexane.

Synthesis of [(η^5-4,7-$Me_2C_9H_5$)Mo(CO)$_2$(NCMe)$_2$][BF_4] (8-BF_4)

[(η^3-C_3H_5)(η^5-4,7-$Me_2C_9H_5$)Mo(CO)$_2$] (**7**; 500 mg, 1.49 mmol) was dissolved in CH_2Cl_2 (50 mL), cooled at 0 °C and treated with acetonitrile (5 mL) and then with $HBF_4 \cdot Et_2O$ (1.49 mmol). The reaction mixture was stirred for one hour at room temperature. Afterwards, the solvent was vacuum evaporated. The crude product was washed with ether and recrystallized from the mixture CH_2Cl_2/ether and vacuum dried. Yield: 608 mg (88%, 1.31 mmol). Orange powder. Mp: 150–160 °C (dec.). Anal. calcd for $C_{17}H_{17}BF_4MoN_2O_2$: C, 44.00; H, 3.69; N, 6.04. Found: C, 43.88; H, 3.73; N, 6.12. ^{1}H NMR (CD_2Cl_2; 400 MHz; δ (ppm)): 7.23 (s, 2H, C_9H_5, H^{5,6}), 6.00 (d, $^3J(^1H,^1H)$ = 2.6 Hz, 2H, C_9H_5, H^{1,3}), 5.01 (t, $^3J(^1H,^1H)$ = 2.6 Hz, 1H, C_9H_5, H^2), 2.36 (s, 6H, CH_3CN), 1.97 (s, 6H, CH_3). FTIR (ATR, cm^{-1}): 1970 vs [ν_a(CO)], 1897 vs [ν_s(CO)], 1040 vs [ν(BF)]. Single crystals of **8-BF_4** suitable for X-ray diffraction analysis were prepared by overlayering of the MeCN solution with Et_2O.

Synthesis of [(η^5-4,7-$Me_2C_9H_5$)Mo(CO)$_2$(bpy)][(η^5-4,7-$Me_2C_9H_5$)-Mo(CO)$_2$Cl$_2$] (4b-9)

[{(η^5-4,7-$Me_2C_9H_5$)Mo(CO)$_2$(μ-Cl)}$_2$] (**2**; 100 mg, 0.15 mmol) was dissolved in CH_2Cl_2 (50 mL) and treated with **bpy** (23 mg, 0.15 mmol). The solution was stirred at room temperature overnight. The precipitate was decanted. The product was washed with ether, CH_2Cl_2 and vacuum dried. Yield: 85 mg (69%, 0.10 mmol). Red powder. Mp: 140–150 °C (dec.). Anal. calcd for $C_{36}H_{30}Cl_2Mo_2N_2O_4$: C, 52.90; H, 3.70; N, 3.43. Found: C, 52.82; H, 3.79; N, 3.51. FTIR (ATR, cm^{-1}): 1950 vs [ν_a(CO)], 1930 vs [ν_a(CO)], 1875 vs [ν_s(CO)], 1837 vs [ν_s(CO)].

Synthesis of [(η^5-4,7-$Me_2C_9H_5$)Mo(CO)$_2$(phen)][(η^5-4,7-$Me_2C_9H_5$)-Mo(CO)$_2$Cl$_2$] (5b-9)

Steps of the synthesis followed the procedure for the compounds **4b-9**. Reagents: [{(η^5-4,7-$Me_2C_9H_5$)Mo(CO)$_2$(μ-Cl)}$_2$] (**2**; 100 mg, 0.15 mmol) and **phen** (27 mg, 0.15 mmol). Yield: 95 mg (75%, 0.11 mmol). Red powder. Mp: 140–150 °C (dec.). Anal. calcd for $C_{38}H_{30}Cl_2Mo_2N_2O_4$: C, 54.24; H, 3.59; N, 3.33. Found: C, 54.38; H, 3.62; N, 3.10. FTIR (ATR, cm^{-1}): 1954 vs [ν_a(CO)], 1926 vs [ν_a(CO)], 1867 vs [ν_s(CO)], 1824 vs [ν_s(CO)]. Single crystals of **5b-9**·CH_2Cl_2 suitable for X-ray diffraction analysis were prepared by overlayering of the CH_2Cl_2 solutions of the starting materials.

Synthesis of [Me_4N][(η^5-4,7-$Me_2C_9H_5$)Mo(CO)$_2$Cl$_2$] (Me_4N-9)

[{(η^5-4,7-$Me_2C_9H_5$)Mo(CO)$_2$(μ-Cl)}$_2$] (**2**; 100 mg, 0.15 mmol) was dissolved in acetone (50 mL) and treated with [Me_4N]Cl (82 mg, 0.75 mmol). The solution was stirred at room temperature overnight. The volatiles were vacuum evaporated. The residuum was dissolved in CH_2Cl_2 and filtered over short pad of Celite. The volatiles were vacuum evaporated. The crude product was washed with ether and recrystallized from the mixture CH_2Cl_2/ether and vacuum dried. Yield: 220 mg (83%, 0.50 mmol). Red powder. Mp: 140–150 °C (dec.). Anal. calcd for $C_{17}H_{23}Cl_2MoNO_2$: C, 46.38; H, 5.27; N, 3.18. Found: C, 46.12; H, 5.32; N, 3.23. ^{1}H NMR ($CDCl_3$; 400 MHz; δ (ppm)): 6.90 (s, 2H, C_9H_5, H^{5,6}), 5.76 (d, $^3J(^1H,^1H)$ = 2.8 Hz, 2H, C_9H_5, H^{1,3}), 4.87 (t, $^3J(^1H,^1H)$ = 2.8 Hz, 1H, C_9H_5, H^2), 3.32 (s, 12H, (CH_3)$_4$N)), 2.29 (s, 6H, (CH_3)$_2$$C_9H_5$)). FTIR (ATR, cm^{-1}): 1936 vs [ν_a(CO)], 1922 vs [ν_a(CO)], 1820 vs [ν_s(CO)].

Synthesis of [(η^3-4,7-$Me_2C_9H_5$)Mo(CO)$_2$(2,9-Me_2-phen)Cl] (10a)

Method A: steps of the synthesis followed the procedure for the compounds **4a**. Reagents: [{(η^5-4,7-$Me_2C_9H_5$)Mo(CO)$_2$(μ-Cl)}$_2$] (**2**; 200 mg, 0.30 mmol) and 2,9-Me_2-phen (125 mg, 0.60 mmol). Yield: 315 mg (97%, 0.58 mmol). Method B: [(η^5-4,7-$Me_2C_9H_5$)-Mo(CO)$_2$(2,9-Me_2-phen)][BF_4] (**10b-BF_4**; 100 mg, 0.20 mmol) was dissolved in acetone (50 mL) and treated with [Me_4N]Cl (220 mg, 2.01 mmol; alternatively 2.01 mmol of NaCl or KCl could be used). The solution was stirred for 48 h. The volatiles were vacuum evaporated. The residuum was dissolved in CH_2Cl_2 and filtered over short pad of Celite. The volatiles were vacuum evaporated. The crude product was washed with ether and recrystallized from the mixture CH_2Cl_2/ether and vacuum dried. Yield: 105 mg (97%, 0.19 mmol). Dark red powder. Mp: 150–160 °C (dec.). Anal. calcd for $C_{27}H_{23}ClMoN_2O_2$: C, 60.18; H, 4.30; N, 5.19. Found: C, 59.96; H, 4.42; N, 5.27. ^{1}H NMR ($CDCl_3$; 400 MHz; δ (ppm)): 8.30 (d, $^3J(^1H,^1H)$ = 8.2 Hz, 2H, $C_{12}H_6N_2$), 7.88 (s, 2H, $C_{12}H_6N_2$), 7.65 (d, $^3J(^1H,^1H)$ = 8.2 Hz, 2H, $C_{12}H_6N_2$), 6.21 (s, 2H, C_9H_5, H^{5,6}), 5.84 (t, $^3J(^1H,^1H)$ = 3.7 Hz, 1H, C_9H_5, H^2), 4.57 (d, $^3J(^1H,^1H)$ = 3.7 Hz, 2H, C_9H_5, H^{1,3}), 3.07 (s, 6H, (CH_3)$_2$$C_{12}H_6N_2$), 2.09 (s, 6H, (C$H_3$)$_2$$C_9H_5$). ^{13}C NMR ($CD_2Cl_2$; 126 MHz; δ (ppm)): 231.0 (2C, *C*O), 162.3, 146.1, 145.9, 129.6, 125.7 (5 × 1C_q), 138.9, 127.1, 126.7, 125.7 (4 × 2C $C_{12}H_6N_2$ and C_9H_5), 103.5 (1C, C^2 of C_9H_5), 69.5 (2C, C^{1,3} of C_9H_5), 28.9 (2C, $C_{12}H_6N_2$(CH_3)$_2$), 17.8 (2C, C_9H_5(CH_3)$_2$). FTIR (ATR, cm^{-1}):

Open Access Article. Published on 16 March 2015. Downloaded on 5/9/2026 9:53:25 AM. This article is licensed under a Creative Commons Attribution-NonCommercial 3.0 Unported Licence.

1927 vs [ν_a(CO)], 1848 vs [ν_s(CO)]. Single crystals of **10a**·CH_2Cl_2 suitable for X-ray diffraction analysis were prepared by overlayering of the CH_2Cl_2 solution with hexane. Single crystals of **10a**·$CHCl_3$ suitable for X-ray diffraction analysis were prepared by overlayering of the $CHCl_3$ solution with ether.

Synthesis of [(η^3-C_3H_5)Mo(CO)$_2$(2,9-Me$_2$-phen)Cl] (10-allyl)

Steps of the synthesis followed the procedure for the compounds **6-allyl**. Reagents: [(η^3-C_3H_5)Mo(CO)$_2$(NCMe)$_2$Cl] (200 mg, 0.64 mmol) and 2,9-Me_2-phen (135 mg, 0.64 mmol). Yield: 260 mg (93%, 0.60 mmol). Dark orange powder. Mp: 150–160 °C (dec.). Anal. calcd for $C_{19}H_{17}ClMoN_2O_2$: C, 52.25; H, 3.92; N, 6.41. Found: C, 52.38; H, 3.86; N, 6.49. ^{1}H NMR (acetone-d^6; 400 MHz; δ (ppm)): 8.60 (d, $^3J(^1H,^1H)$ = 8.3 Hz, 2H, $C_{12}H_6N_2$), 8.07 (s, 2H, $C_{12}H_6N_2$), 7.93 (d, $^3J(^1H,^1H)$ = 8.3 Hz, 2H, $C_{12}H_6N_2$), 3.27 (s, 6H, CH_3), 2.69 (d, $^3J(^1H,^1H)$ = 6.2 Hz, 2H, *syn*-C_3H_5), 2.63 (tt, 1H, *meso*-C_3H_5), 1.13 (d, $^3J(^1H,^1H)$ = 9.0 Hz, 2H, *anti*-C_3H_5). FTIR (ATR, cm^{-1}): 1929 vs [ν_a(CO)], 1836 vs [ν_s(CO)]. Single crystals of **10-allyl** suitable for X-ray diffraction analysis were prepared by overlayering of the CH_2Cl_2 solution with hexane.

Synthesis of [(η^5-4,7-Me$_2$C$_9$H$_5$)Mo(CO)$_2$(2,9-Me$_2$-phen)][BF$_4$] (10b-BF$_4$)

Steps of the synthesis followed the procedure for the compounds **4b-BF$_4$**. Reagents: [(η^5-4,7-$Me_2C_9H_5$)Mo(CO)$_2$(NCMe)$_2$][BF_4] (**8-BF$_4$**; 500 mg, 1.08 mmol) and 2,9-Me_2-phen (224 mg, 1.08 mmol). Yield: 505 mg (96%, 1.03 mmol). Red powder. Mp: 160–170 °C (dec.). Anal. calcd for $C_{19}H_{17}BF_4MoN_2O_2$: C, 46.75; H, 3.51; N, 5.74. Found: C, 46.92; H, 3.35; N, 5.78. ^{1}H NMR (CD_2Cl_2; 400 MHz; δ (ppm)): 8.50 (d, $^3J(^1H,^1H)$ = 8.3 Hz, 2H, $C_{12}H_6N_2$), 7.96 (s, 2H, $C_{12}H_6N_2$), 7.86 (d, $^3J(^1H,^1H)$ = 8.3 Hz, 2H, $C_{12}H_6N_2$), 6.27 (d, $^3J(^1H,^1H)$ = 2.9 Hz, 2H, C_9H_5, $H^{1,3}$), 6.04 (s, 2H, C_9H_5, $H^{5,6}$), 5.45 (t, $^3J(^1H,^1H)$ = 2.9 Hz, 1H, C_9H_5, H^2), 3.60 (s, 6H, $(CH_3)_2C_{12}H_6N_2$), 1.74 (s, 6H, $(CH_3)_2C_9H_5$). ^{13}C NMR (CD_2Cl_2; 101 MHz; δ (ppm)): 252.5 (2C, *C*O), 166.5, 146.2, 132.9, 131.5, 121.0 (5 × 1C_q), 140.2, 130.0, 127.3, 127.3 (4 × 2C $C_{12}H_6N_2$ and C_9H_5), 90.6 (1C, C^2 of C_9H_5), 79.9 (2C, $C^{1,3}$ of C_9H_5), 32.8 (2C, $C_{12}H_6N_2(CH_3)_2$), 18.6 (2C, $C_9H_5(CH_3)_2$). FTIR (ATR, cm^{-1}): 1946 vs [ν_a(CO)], 1867 vs [ν_s(CO)]. Single crystals of **10b-BF$_4$**·0.5(Me_2-phen·HBF_4) suitable for X-ray diffraction analysis were prepared by overlayering of the crude product in CH_2Cl_2 with hexane.

Synthesis of [(η^3-4,7-Me$_2$C$_9$H$_5$)Mo(CO)$_2$(2,9-Me$_2$-phen)Br] (10c)

Steps of the synthesis followed the procedure for the compounds **10a** (Method B). Reagents: [(η^5-4,7-$Me_2C_9H_5$)-Mo(CO)$_2$(2,9-Me$_2$-phen)][BF_4] (**10b-BF$_4$**; 100 mg, 0.20 mmol) and KBr (240 mg, 2.02 mmol). Yield: 90 mg (94%, 0.19 mmol). Dark red powder. Mp: 160–170 °C (dec.). Anal. calcd for $C_{19}H_{17}BrMoN_2O_2$: C, 47.42; H, 3.56; N, 5.82. Found: C, 47.30; H, 3.62; N, 5.95. ^{1}H NMR ($CDCl_3$; 400 MHz; δ (ppm)): 8.30 (d, $^3J(^1H,^1H)$ = 8.3 Hz, 2H, $C_{12}H_6N_2$), 7.89 (s, 2H, $C_{12}H_6N_2$), 7.65 (d, $^3J(^1H,^1H)$ = 8.3 Hz, 2H, $C_{12}H_6N_2$), 6.21 (s, 2H, C_9H_5, $H^{5,6}$), 5.83 (t, $^3J(^1H,^1H)$ = 3.7 Hz, 1H, C_9H_5, H^2), 4.61 (d, $^3J(^1H,^1H)$ = 3.7 Hz, 2H, C_9H_5, $H^{1,3}$), 3.04 (s, 6H, $(CH_3)_2C_{12}H_6N_2$), 2.08 (s, 6H, $(CH_3)_2C_9H_5$). ^{13}C NMR (CD_2Cl_2; 101 MHz; δ (ppm)): 230.1 (2C, *C*O), 162.6, 146.2, 145.9, 129.7, 125.8 (5 × 1C_q), 138.8, 127.1, 126.6, 125.9 (4 × 2C $C_{12}H_6N_2$ and C_9H_5), 103.6 (1C, C^2 of C_9H_5), 68.6 (2C, $C^{1,3}$ of C_9H_5), 30.1 (2C, $C_{12}H_6N_2(CH_3)_2$), 17.8 (2C, $C_9H_5(CH_3)_2$). FTIR (ATR, cm^{-1}): 1936 vs [ν_a(CO)], 1863 vs [ν_s(CO)]. Single crystals of **10c** suitable for X-ray diffraction analysis were prepared by overlayering of the CH_2Cl_2 solution with Et_2O.

Synthesis of [(η^3-4,7-Me$_2$C$_9$H$_5$)Mo(CO)$_2$(2,9-Me$_2$-phen)I] (10d)

Steps of the synthesis followed the procedure for the compounds **10a** (Method B). Reagents: [(η^5-4,7-$Me_2C_9H_5$)-Mo(CO)$_2$(2,9-Me$_2$-phen)][BF_4] (**10b-BF$_4$**; 100 mg, 0.20 mmol) and KI (330 mg, 1.99 mmol). Yield: 100 mg (95%, 0.19 mmol). Brown powder. Mp: 160–170 °C (dec.). Anal. calcd for $C_{19}H_{17}IMoN_2O_2$: C, 43.20; H, 3.24; N, 5.30. Found: C, 43.44; H, 3.34; N, 5.43. ^{1}H NMR ($CDCl_3$; 400 MHz; δ (ppm)): 8.29 (d, $^3J(^1H,^1H)$ = 8.2 Hz, 2H, $C_{12}H_6N_2$), 7.91 (s, 2H, $C_{12}H_6N_2$), 7.65 (d, $^3J(^1H,^1H)$ = 8.2 Hz, 2H, $C_{12}H_6N_2$), 6.21 (s, 2H, C_9H_5, $H^{5,6}$), 5.84 (s-br, 1H, C_9H_5, H^2), 4.69 (d, $^3J(^1H,^1H)$ = 3.4 Hz, 2H, C_9H_5, $H^{1,3}$), 3.00 (s, 6H, $(CH_3)_2C_{12}H_6N_2$), 2.07 (s, 6H, $(CH_3)_2C_9H_5$). ^{13}C NMR (CD_2Cl_2; 126 MHz; δ (ppm)): 229.0 (2C, *C*O), 162.9, 146.3, 145.8, 129.8, 125.9 (5 × 1C_q), 138.8, 127.2, 126.5, 125.9 (4 × 2C $C_{12}H_6N_2$ and C_9H_5), 104.3 (1C, C^2 of C_9H_5), 67.5 (2C, $C^{1,3}$ of C_9H_5), 30.5 (2C, $C_{12}H_6N_2(CH_3)_2$), 17.9 (2C, $C_9H_5(CH_3)_2$). FTIR (ATR, cm^{-1}): 1932 vs [ν_a(CO)], 1861 vs [ν_s(CO)].

Synthesis of [(η^3-4,7-Me$_2$C$_9$H$_5$)Mo(CO)$_2$(2,9-Me$_2$-phen)(NCO)] (10e)

Steps of the synthesis followed the procedure for the compounds **10a** (Method B). Reagents: [(η^5-4,7-$Me_2C_9H_5$)-Mo(CO)$_2$(2,9-Me$_2$-phen)][BF_4] (**10b-BF$_4$**; 100 mg, 0.20 mmol) and KOCN (160 mg, 1.97 mmol). Yield: 80 mg (90%, 0.18 mmol). Dark red powder. Mp: 160–170 °C (dec.). Anal. calcd for $C_{20}H_{17}MoN_3O_3$: C, 54.19; H, 3.87; N, 9.48. Found: C, 54.01; H, 3.89; N, 9.32. ^{1}H NMR ($CDCl_3$; 400 MHz; δ (ppm)): 8.34 (d, $^3J(^1H,^1H)$ = 8.3 Hz, 2H, $C_{12}H_6N_2$), 7.94 (s, 2H, $C_{12}H_6N_2$), 7.71 (d, $^3J(^1H,^1H)$ = 8.3 Hz, 2H, $C_{12}H_6N_2$), 6.20 (s, 2H, C_9H_5, $H^{5,6}$), 5.88 (t, $^3J(^1H,^1H)$ = 3.7 Hz, 1H, C_9H_5, H^2), 4.68 (d, $^3J(^1H,^1H)$ = 3.7 Hz, 2H, C_9H_5, $H^{1,3}$), 3.02 (s, 6H, $(CH_3)_2C_{12}H_6N_2$), 2.08 (s, 6H, $(CH_3)_2C_9H_5$). FTIR (ATR, cm^{-1}): 2195 vs [ν(CN)], 1930 vs [ν_a(CO)], 1851 vs [ν_s(CO)].

Synthesis of [(η^3-4,7-Me$_2$C$_9$H$_5$)Mo(CO)$_2$(2,9-Me$_2$-phen)(NCS)] (10f)

Steps of the synthesis followed the procedure for the compounds **10a** (Method B). Reagents: [(η^5-4,7-$Me_2C_9H_5$)-Mo(CO)$_2$(2,9-Me$_2$-phen)][BF_4] (**10b-BF$_4$**; 100 mg, 0.20 mmol) and KSCN (200 mg, 2.06 mmol). Yield: 90 mg (98%, 0.19 mmol). Red powder. Mp: 150–160 °C (dec.). Anal. calcd for $C_{20}H_{17}MoN_3O_2S$: C, 52.29; H, 3.73; N, 9.15, S, 6.98. Found: C, 52.09; H, 3.65; N, 9.00, S, 7.12. ^{1}H NMR ($CDCl_3$; 400 MHz; δ (ppm)): 8.42 (d, $^3J(^1H,^1H)$ = 8.3 Hz, 2H, $C_{12}H_6N_2$), 7.96 (s, 2H, $C_{12}H_6N_2$), 7.73 (d, $^3J(^1H,^1H)$ = 8.3 Hz, 2H, $C_{12}H_6N_2$), 6.21 (s, 2H, C_9H_5, $H^{5,6}$), 5.79 (t, $^3J(^1H,^1H)$ = 3.7 Hz, 1H, C_9H_5, H^2), 4.77 (d, $^3J(^1H,^1H)$ = 3.7 Hz, 2H, C_9H_5, $H^{1,3}$), 3.04 (s, 6H, $(CH_3)_2C_{12}H_6N_2$), 2.08 (s, 6H,

 This journal is © The Royal Society of Chemistry 2015

Open Access Article. Published on 16 March 2015. Downloaded on 5/9/2026 9:53:25 AM.
This article is licensed under a Creative Commons Attribution-NonCommercial 3.0 Unported Licence.

$(CH_3)_2C_9H_5$). FTIR (ATR, cm^{-1}): 2063 vs [ν(CN)], 1925 vs [ν_a(CO)], 1849 vs [ν_s(CO)].

Synthesis of [(η^3-4,7-$Me_2C_9H_5$)Mo(CO)$_2$(3,4,7,8-Me_4-phen)Cl] (11a)

Steps of the synthesis followed the procedure for the compounds **4a**. Reagents: [{(η^5-4,7-$Me_2C_9H_5$)Mo(CO)$_2$(μ-Cl)}$_2$] (**2**; 50 mg, 76 μmol) and 3,4,7,8-Me_4-phen (35 mg, 0.15 mmol). Yield: 50 mg (93%, 88 μmol). Red powder. Mp: 140–150 °C (dec.). Anal. calcd for $C_{25}H_{21}ClMoN_2O_2$: C, 61.44; H, 4.80; N, 5.64. Found: C, 61.28; H, 4.87; N, 5.55. ^{1}H NMR (CD_2Cl_2; 400 MHz; δ (ppm); **11a** and **11b-Cl** in the ratio 1 : 3): 9.13 (s, 2H of **b**, $C_{12}H_4N_2$), 8.59 (s, 2H of **a**, $C_{12}H_4N_2$), 8.17 (s, 2H of **b**, $C_{12}H_4N_2$), 8.14 (s, 2H of **a**, $C_{12}H_4N_2$), 6.32 (d, $^3J(^1H,^1H) = 2.8$ Hz, 2H of **b**, C_9H_5, $H^{1,3}$), 6.28 (s, 2H of **b**, C_9H_5, $H^{5,6}$), 6.22 (t, $^3J(^1H,^1H) = 3.7$ Hz, 1H of **a**, C_9H_5, H^2), 6.21 (s, 2H of **a**, C_9H_5, $H^{5,6}$), 5.70 (t, $^3J(^1H,^1H) = 2.8$ Hz, 1H of **b**, C_9H_5, H^2), 4.93 (d, $^3J(^1H,^1H) = 3.7$ Hz, 2H of **a**, C_9H_5, $H^{1,3}$), 2.82 (s, 6H of **b**, $(CH_3)_4C_{12}H_4N_2$), 2.76 (s, 6H of **a**, $(CH_3)_4C_{12}H_4N_2$), 2.66 (s, 6H of **b**, $(CH_3)_4C_{12}H_4N_2$), 2.58 (s, 6H of **a**, $(CH_3)_4C_{12}H_4N_2$), 2.16 (s, 6H of **a**, $(CH_3)_2C_9H_5$), 1.88 (s, 6H of **b**, $(CH_3)_2C_9H_5$). FTIR (ATR, cm^{-1}): 1922 vs [ν_a(CO)], 1839 *vs* [ν_s(CO)].

Synthesis of [(η^3-4,7-$Me_2C_9H_5$)Mo(CO)$_2$(2,9-Me_2-4,7-Ph_2-phen)Cl] (12a)

Steps of the synthesis followed the procedure for the compounds **10a** (Method B). Reagents: [(η^5-4,7-$Me_2C_9H_5$)-Mo(CO)$_2$(2,9-Me_2-4,7-Ph_2-phen)][BF_4] (**12b-BF_4**; 30 mg, 40 μmol) and [Me_4N]Cl (44 mg, 0.40 mmol). Yield: 27 mg (97%, 39 μmol). Purple powder. Mp: 170–180 °C (dec.). Anal. calcd for $C_{39}H_{31}ClMoN_2O_2$: C, 67.78; H, 4.52; N, 4.05. Found: C, 67.89; H, 4.47; N, 4.19. ^{1}H NMR (CD_2Cl_2; 500 MHz; δ (ppm)): 7.94 (s, 2H, $C_{12}H_4N_2$), 7.66 (s, 2H, $C_{12}H_4N_2$), 7.62–7.55 (m, 10H, C_6H_5), 6.21 (s, 2H, C_9H_5, $H^{5,6}$), 6.07 (t, $^3J(^1H,^1H) = 3.7$ Hz, 1H, C_9H_5, H^2), 4.70 (d, $^3J(^1H,^1H) = 3.7$ Hz, 2H, C_9H_5, $H^{1,3}$), 3.07 (s, 6H, $(CH_3)_2C_{12}H_4N_2$), 2.10 (s, 6H, $(CH_3)_2C_9H_5$). ^{13}C NMR (CD_2Cl_2; 126 MHz; δ (ppm)): 231.1 (2C, *C*O), 161.5, 151.2, 146.7, 146.1, 136.9, 127.8, 125.7 (7 × 1C_q), 130.1, 129.4 (2 × 4C C_6H_5), 129.8, 127.1, 125.7, 124.8 (4 × 2C $C_{12}H_4N_2$, C_6H_5 and C_9H_5), 103.8 (1C, C^2 of C_9H_5), 69.4 (2C, $C^{1,3}$ of C_9H_5), 30.1 (2C, $C_{12}H_4N_2(CH_3)_2$), 17.8 (2C, $C_9H_5(CH_3)_2$). FTIR (ATR, cm^{-1}): 1939 vs [ν_a(CO)], 1862 vs [ν_s(CO)].

Synthesis of [(η^5-4,7-$Me_2C_9H_5$)Mo(CO)$_2$(2,9-Me_2-4,7-Ph_2-phen)][BF_4] (12b-BF_4)

Steps of the synthesis followed the procedure for the compounds **4b-BF_4**. Reagents: [(η^5-4,7-$Me_2C_9H_5$)Mo(CO)$_2$-(NCMe)$_2$][BF_4] (**8-BF_4**; 50 mg, 0.11 mmol) and 2,9-Me_2-4,7-Ph_2-phen (36 mg, 0.11 mmol). Yield: 78 mg (98%, 0.11 mmol). Red powder. Mp: 150–160 °C (dec.). Anal. Calcd for $C_{39}H_{31}BF_4MoN_2O_2$: C, 63.09; H, 4.21; N, 3.77. Found: C, 63.25; H, 4.14; N, 3.89. ^{1}H NMR (CD_2Cl_2; 500 MHz; δ (ppm)): 7.94 (s, 2H, $C_{12}H_4N_2$), 7.82 (s, 2H, $C_{12}H_4N_2$), 7.66–7.52 (m, 10H, C_6H_5), 4.31 (d, $^3J(^1H,^1H) = 2.8$ Hz, 2H, C_9H_5, $H^{1,3}$), 6.11 (s, 2H, C_9H_5, $H^{5,6}$), 5.49 (t, $^3J(^1H,^1H) = 2.8$ Hz, 1H, C_9H_5, H^2), 3.63 (s, 6H, $(CH_3)_2C_{12}H_4N_2$), 1.79 (s, 6H, $(CH_3)_2C_9H_5$). ^{13}C NMR (CD_2Cl_2; 126 MHz; δ (ppm)): 252.4 (2C, *C*O), 166.0, 152.1, 147.1, 135.7, 133.0, 121.3 (6 × 1C_q), 130.0, 129.8 (2 × 4C C_6H_5), 130.7, 129.8, 127.6, 124.9 (4 × 2C $C_{12}H_4N_2$, C_6H_5 and C_9H_5), 91.1 (1C, C^2 of C_9H_5), 79.8 (2C, $C^{1,3}$ of C_9H_5), 33.1 (2C, $C_{12}H_4N_2(CH_3)_2$), 18.8 (2C, $C_9H_5(CH_3)_2$). FTIR (ATR, cm^{-1}): 1944 vs [ν_a(CO)], 1893 s [ν_s(CO)], 1877 s [ν_s(CO)].

Synthesis of [(η^5-4,7-$Me_2C_9H_5$)Mo(CO)$_2$(4,4′-Me_2-bpy)][Cl] (13b-Cl)

Steps of the synthesis followed the procedure for the compounds **4a**. Reagents: [{(η^5-4,7-$Me_2C_9H_5$)Mo(CO)$_2$(μ-Cl)}$_2$] (**2**; 50 mg, 76 μmol) and 4,4′-Me_2-bpy (28 mg, 0.15 mmol). Yield: 75 mg (96%, 0.15 mmol). Red powder. Mp: 130–140 °C (dec.). Anal. calcd for $C_{25}H_{23}ClMoN_2O_2$: C, 58.32; H, 4.50; N, 5.44. Found: C, 58.45; H, 4.61; N, 5.52. ^{1}H NMR (CD_2Cl_2; 400 MHz; δ (ppm)): 8.84 (d, $^3J(^1H,^1H) = 5.4$ Hz, 2H, $C_{10}H_6N_2$), 8.72 (s, 2H, $C_{10}H_6N_2$), 7.32 (d, $^3J(^1H,^1H) = 5.4$ Hz, 2H, $C_{10}H_6N_2$), 6.60 (s, 2H, C_9H_5, $H^{5,6}$), 6.16 (s-br, C_9H_5, $H^{1,3}$), 5.55 (s-br, 1H, C_9H_5, H^2), 2.62 (s, 6H, $(CH_3)_2C_{10}H_6N_2$), 1.96 (s, 6H, $(CH_3)_2C_9H_5$). FTIR (ATR, cm^{-1}): 1962 vs [ν_a(CO)], 1877 vs [ν_s(CO)].

Synthesis of [(η^3-4,7-$Me_2C_9H_5$)Mo(CO)$_2$(6,6′-Me_2-bpy)Cl] (14a)

Steps of the synthesis followed the procedure for the compounds **10a** (Method B). Reagents: [(η^5-4,7-$Me_2C_9H_5$)-Mo(CO)$_2$(6,6′-Me_2-bpy)][BF_4] (**14b-BF_4**; 30 mg, 53 μmol) and [Me_4N]Cl (58 mg, 0.53 mmol). Yield: 27 mg (99%, 52 μmol). Purple powder. Mp: 170–180 °C (dec.). Anal. calcd for $C_{25}H_{23}ClMoN_2O_2$: C, 58.32; H, 4.50; N, 5.44. Found: C, 58.39; H, 4.56; N, 5.45. ^{1}H NMR (CD_2Cl_2; 400 MHz; δ (ppm)): 8.09 (d, $^3J(^1H,^1H) = 7.8$ Hz, 2H, $C_{10}H_6N_2$), 7.91 (dd, $^3J(^1H,^1H) = 7.8$ Hz, $^3J(^1H,^1H) = 7.6$ Hz, 2H, $C_{10}H_6N_2$), 7.40 (d, $^3J(^1H,^1H) = 7.6$ Hz, 2H, $C_{10}H_6N_2$), 6.18 (s, 2H, C_9H_5, $H^{5,6}$), 6.09 (t, $^3J(^1H,^1H) = 3.7$ Hz, 1H, C_9H_5, H^2), 4.55 (d, $^3J(^1H,^1H) = 3.7$ Hz, 2H, C_9H_5, $H^{1,3}$), 2.79 (s, 6H, $(CH_3)_2C_{10}H_6N_2$), 2.05 (s, 6H, $(CH_3)_2C_9H_5$). FTIR (ATR, cm^{-1}): 1930 vs [ν_a(CO)], 1852 vs [ν_s(CO)].

Synthesis of [(η^5-4,7-$Me_2C_9H_5$)Mo(CO)$_2$(6,6′-Me_2-bpy)][BF_4] (14b-BF_4)

Steps of the synthesis followed the procedure for the compounds **4b-BF_4**. Reagents: [(η^5-4,7-$Me_2C_9H_5$)Mo(CO)$_2$-(NCMe)$_2$][BF_4] (**8-BF_4**; 50 mg, 0.11 mmol) and 6,6′-Me_2-bpy (20 mg, 0.11 mmol). Yield: 60 mg (98%, 0.11 mmol). Red powder. Mp: 160–170 °C (dec.). Anal. calcd for $C_{25}H_{23}BF_4$-MoN_2O_2: C, 53.03; H, 4.09; N, 5.95. Found: C, 53.10; H, 4.12; N, 5.92. ^{1}H NMR (CD_2Cl_2; 400 MHz; δ (ppm)): 8.15 (d, $^3J(^1H,^1H) = 8.0$ Hz, 2H, $C_{10}H_6N_2$), 7.99 (dd, $^3J(^1H,^1H) = 8.0$ Hz, $^3J(^1H,^1H) = 7.6$ Hz, 2H, $C_{10}H_6N_2$), 7.52 (dd, $^3J(^1H,^1H) = 7.6$ Hz, $^4J(^1H,^1H) = 1.0$ Hz, 2H, $C_{10}H_6N_2$), 6.55 (s, 2H, C_9H_5, $H^{5,6}$), 6.19 (d, $^3J(^1H,^1H) = 2.9$ Hz, 2H, C_9H_5, $H^{1,3}$), 5.31 (t, $^3J(^1H,^1H) = 2.9$ Hz, 1H, C_9H_5, H^2), 3.35 (s, 6H, $(CH_3)_2C_{10}H_6N_2$), 1.84 (s, 6H, $(CH_3)_2C_9H_5$). FTIR (ATR, cm^{-1}): 1947 vs [ν_a(CO)], 1870 vs [ν_s(CO)].

X-ray crystallography

The X-ray data for the crystals of the compounds **3**, **4b-BF_4**, **5b-9**·CH_2Cl_2, **6a**, **6-allyl**, **8-BF_4**, **10a**·CH_2Cl_2, **10a**·$CHCl_3$, **10-allyl**,

Open Access Article. Published on 16 March 2015. Downloaded on 5/9/2026 9:53:25 AM. This article is licensed under a Creative Commons Attribution-NonCommercial 3.0 Unported Licence.

10b-BF_4·0.5(phen·HBF_4) and **10c** and were obtained at 150 K using an Oxford Cryostream low-temperature device on a Nonius KappaCCD diffractometer with Mo Kα radiation (λ = 0.71073 Å) and a graphite monochromator. Data reductions were performed with DENZO-SMN.[64] The absorption was corrected by integration methods[65] and only in cases of **5b-9**·CH_2Cl_2 and **6a** it was performed analytically using SADABS software.[66] Structures were solved by direct methods (Sir92)[67] and refined by full-matrix least squares based on F^2 (SHELXL).[68] Thermal ellipsoids of C13 and C14 atoms in **5b-9**·CH_2Cl_2, of F1, F3 and F4 atoms in **8-BF_4** and of F1 atom in **10b-BF_4**·0.5(phen·HBF_4) were treated with standard ISOR instruction implemented in SHELXL97 software.[68] Hydrogen atoms were mostly localized on a difference Fourier map. However, to ensure uniformity of the treatment of the crystal, all hydrogen atoms were recalculated into idealized positions (riding model) and assigned temperature factors $U_{iso}(H) = 1.2[U_{eq}(\text{pivot atom})]$ or $1.5U_{eq}$ for the methyl moiety with C–H = 0.96, 0.97, and 0.93 Å for methyl, methylene, and hydrogen atoms in aromatic rings or the allyl moiety, respectively.

Acknowledgements

This work was supported by Ministry of Education of the Czech Republic (Project no. SG350004).

References

1 E. Hevia, J. Pérez, L. Riera, V. Riera, I. del Río, S. García-Granda and D. Miguel, *Chem.–Eur. J.*, 2002, **8**, 4510–4521.
2 L. Coue, L. Cuesta, D. Morales, J. A. Halfen, J. Pérez, L. Riera, V. Riera, D. Miguel, N. G. Connelly and S. Boonyuen, *Chem.–Eur. J.*, 2004, **10**, 1906–1912.
3 J. Pérez, L. Riera, V. Riera, S. García-Granda, E. García-Rodríguez and D. Miguel, *Chem. Commun.*, 2002, 384–385.
4 D. Morales, J. Pérez, L. Riera, V. Riera, D. Miguel, M. E. G. Mosquera and S. García-Granda, *Chem.–Eur. J.*, 2003, **9**, 4132–4143.
5 D. Morales, M. E. N. Clemente, J. Pérez, L. Riera, V. Riera and D. Miguel, *Organometallics*, 2003, **22**, 4124–4128.
6 E. Hevia, J. Pérez, L. Riera, V. Riera and D. Miguel, *Organometallics*, 2002, **21**, 1750–1752.
7 J. Pérez, L. Riera, V. Riera, S. García-Granda, E. García-Rodríguez and D. Miguel, *Organometallics*, 2002, **21**, 1622–1626.
8 W. Chen, K. Sana, Y. Jiang, E. V. S. Meyer, S. Lapp, M. R. Galinski and L. S. Liebeskind, *Organometallics*, 2013, **32**, 7594–7611.
9 T. C. Coombs, W. Huang, E. C. Garnier-Amblard and L. S. Liebeskind, *Organometallics*, 2010, **29**, 5083–5097.
10 J. C. Alonso, P. Neves, M. J. P. da Silva, S. Quintal, P. D. Vaz, C. Silva, A. A. Valente, P. Ferreira, M. J. Calhorda, V. Félix and M. G. B. Drew, *Organometallics*, 2007, **26**, 5548–5556.
11 C. A. Gamelas, A. C. Gomes, S. M. Bruno, F. A. A. Paz, A. A. Valente, M. Pillinger, C. C. Romão and I. S. Gonçalves, *Dalton Trans.*, 2012, 3474–3484.
12 M. R. P. Norton de Matos, C. C. Romão, C. C. L. Pereira, S. S. Rodrigues, M. Mora, M. J. P. Silva, P. M. Alves and C. A. Reis, International Patent WO/2005/087783, 2005.
13 J. Honzíček, J. Vinklárek, Z. Padělková, L. Šebestová, K. Foltánová and M. Řezáčová, *J. Organomet. Chem.*, 2012, **716**, 258–268.
14 J. Honzíček, J. Vinklárek, M. Erben, Z. Padělková, L. Šebestová and M. Řezáčová, *J. Organomet. Chem.*, 2014, **749**, 387–393.
15 M. Abrantes, A. M. Santos, J. Mink, F. E. Kühn and C. C. Romão, *Organometallics*, 2003, **22**, 2112–2118.
16 S. Huber, M. Cokoja and F. E. Kühn, *J. Organomet. Chem.*, 2014, **751**, 25–32.
17 M. Abrantes, S. Gago, A. A. Valente, M. Pillinger, I. S. Gonçalves, T. M. Santos, J. Rocha and C. C. Romão, *Eur. J. Inorg. Chem.*, 2004, 4914–4920.
18 A. Capapé, A. Raith, E. Herdtweck, M. Cokoja and F. E. Kühn, *Adv. Synth. Catal.*, 2010, **352**, 547–556.
19 S. Li, C. W. Kee, K. W. Huang, T. S. A. Hor and J. Zhao, *Organometallics*, 2010, **29**, 1924–1933.
20 C. A. Gamelas, T. Lourenço, A. P. da Costa, A. L. Simplício, B. Royo and C. C. Romão, *Tetrahedron Lett.*, 2008, **49**, 4708–4712.
21 L. F. Veiros, C. A. Gamelas, M. J. Calhorda and C. C. Romão, *Organometallics*, 2011, **30**, 1454–1465.
22 J. Honzíček, J. Vinklárek, M. Erben, J. Lodinský, L. Dostál and Z. Padělková, *Organometallics*, 2013, **32**, 3502–3511.
23 S. M. Bruno, A. C. Gomes, C. A. Gamelas, M. Abrantes, M. C. Oliveira, A. A. Valente, F. A. A. Paz, M. Pillinger, C. C. Romão and I. S. Gonçalves, *New J. Chem.*, 2014, **38**, 3172–3180.
24 A. C. Gomes, C. A. Gamelas, J. A. Fernandes, F. A. A. Paz, P. Nunes, M. Pillinger, I. S. Gonçalves, C. C. Romão and M. Abrantes, *Eur. J. Inorg. Chem.*, 2014, 3681–3689.
25 J. M. O'Connor and C. P. Casey, *Chem. Rev.*, 1987, **87**, 307–318.
26 H. Bang, T. J. Lynch and F. Basolo, *Organometallics*, 1992, **11**, 40–48.
27 M. E. Rerek, L. N. Ji and F. Basolo, *J. Chem. Soc., Chem. Commun.*, 1983, 1208–1209.
28 C. P. Casey and J. M. O'Connor, *Organometallics*, 1985, **4**, 384–388.
29 J. S. Merola, R. T. Kacmarcik and D. Van Engent, *J. Am. Chem. Soc.*, 1986, **108**, 329–331.
30 C. C. Romão, *Appl. Organomet. Chem.*, 2000, **14**, 539–548.
31 M. J. Calhorda, C. C. Romão and L. F. Veiros, *Chem.–Eur. J.*, 2002, **8**, 868–875.
32 M. J. Calhorda and L. F. Veiros, *Coord. Chem. Rev.*, 1999, **185–186**, 37–51.
33 C. A. Gamelas, N. A. G. Bandeira, C. C. L. Pereira, M. J. Calhorda, E. Herdtweck, M. Machuqueiro, C. C. Romão and L. F. Veiros, *Dalton Trans.*, 2011, 10513–10525.
34 J. Honzíček, F. A. A. Paz and C. C. Romão, *Eur. J. Inorg. Chem.*, 2007, 2827–2838.

 This journal is © The Royal Society of Chemistry 2015

Open Access Article. Published on 16 March 2015. Downloaded on 5/9/2026 9:53:25 AM.
This article is licensed under a Creative Commons Attribution-NonCommercial 3.0 Unported Licence.

35 J. Honzíček, C. C. Romão, M. J. Calhorda, A. Mukhopadhyay, J. Vinklárek and Z. Padělková, *Organometallics*, 2011, **30**, 717–725.
36 O. J. Curnow and G. M. Fern, *J. Organomet. Chem.*, 2005, **690**, 3018–3026.
37 M. B. Meredith, J. A. Crisp, E. D. Brady, T. P. Hanusa, G. T. Yee, M. Pink, W. W. Brennessel and V. G. Young, *Organometallics*, 2008, **27**, 5464–5473.
38 R. B. King and K. N. Chen, *Inorg. Chem.*, 1977, **16**, 3372–3376.
39 J. Honzíček, A. Mukhopadhyay and C. C. Romão, *Inorg. Chim. Acta*, 2010, **363**, 1601–1603.
40 M. J. Calhorda, C. A. Gamelas, I. S. Gonçalves, E. Herdtweck, C. C. Romão and L. F. Veiros, *Organometallics*, 1998, **17**, 2597–2611.
41 J. W. Faller, R. H. Crabtree and A. Habib, *Organometallics*, 1985, **4**, 929–935.
42 J. Honzíček, I. Honzíčková, J. Vinklárek and Z. Růžičková, *J. Organomet. Chem.*, 2014, **772–773**, 299–306.
43 C. A. Gamelas, E. Herdtweck, J. P. Lopes and C. C. Romão, *Organometallics*, 1999, **18**, 506–515.
44 C. C. L. Pereira, P. J. Costa, M. J. Calhorda, C. Freire, S. S. Rodrigues, E. Herdtweck and C. C. Romão, *Organometallics*, 2006, **25**, 5223–5234.
45 J. Honzíček, A. Mukhopadhyay, T. S. Silva, M. J. Romão and C. C. Romão, *Organometallics*, 2009, **28**, 2871–2879.
46 J. Schejbal, J. Honzíček, J. Vinklárek, M. Erben and Z. Růžičková, *Eur. J. Inorg. Chem.*, 2014, 5895–5907.
47 A. Bondi, *J. Phys. Chem.*, 1964, **68**, 441–451.
48 One referee suggested that this π–π stacking may be responsible for folding of the chelate cycle instead of the described repulsion forces. Since it is difficult to separate these two factors, it is subject of our ongoing deeper investigation.
49 J. W. Faller, D. A. Haitko, R. D. Adams and D. F. Chodosh, *J. Am. Chem. Soc.*, 1979, **101**, 865–876.
50 C. G. Hull and M. H. B. Stiddard, *J. Organomet. Chem.*, 1967, **9**, 519–525.
51 A. J. Graham and R. H. Fenn, *J. Organomet. Chem.*, 1970, **25**, 173–191.
52 N. W. Murrall and A. J. Welch, *J. Organomet. Chem.*, 1986, **301**, 109–130.
53 W. Goodyear, C. W. Hemingway, R. W. Harrington, M. R. Wiseman and B. J. Brisdon, *J. Organomet. Chem.*, 2002, **664**, 176–181.
54 J. R. Ascenso, C. G. de Azevedo, M. J. Calhorda, M. A. A. F. d. C. T. Carrondo, P. Costa, A. R. Dias, M. G. B. Drew, V. Félix, A. M. Galvão and C. C. Romão, *J. Organomet. Chem.*, 2001, **632**, 197–208.
55 G. G. Siegel and T. Zeegers-Huyskens, *Spectrochim. Acta, Part A*, 1989, **45**, 1297–1304.
56 C. Crotti, E. Farnetti, S. Filipuzzi, M. Stener, E. Zangrando and P. Moras, *Dalton Trans.*, 2007, 133–142.
57 D. J. Mindiola, *Acc. Chem. Res.*, 2006, **39**, 813–821.
58 P. L. Holland, *Acc. Chem. Res.*, 2008, **41**, 905–914.
59 P. P. Power, *J. Organomet. Chem.*, 2004, **689**, 3904–3919.
60 P. J. Chirik, *Organometallics*, 2010, **29**, 1500–1517.
61 W. L. F. Armarego and D. D. Perrin, in *Purification of Laboratory Chemicals*, Oxford, 1996.
62 J. W. Faller, C. C. Chen, M. J. Mattina and A. Jakubowski, *J. Organomet. Chem.*, 1973, **52**, 361–386.
63 L. Y. Liao, X. R. Kong and X. F. Duan, *J. Org. Chem.*, 2014, **79**, 777–782.
64 Z. Otwinowski and W. Minor, *Methods Enzymol.*, 1997, **276**, 307–326.
65 P. Coppens, in *Crystallographic Computing*, ed. F. R. Ahmed, S. R. Hall and C. P. Huber, Copenhagen, 1970.
66 G. M. Sheldrick, in *SADABS*, Bruker AXS Inc., Madison, Wisconsin, USA, 2002.
67 A. Altomare, G. Cascarano, C. Giacovazzo, A. Guagliardi, M. C. Burla, G. Polidori and M. Camalli, *J. Appl. Crystallogr.*, 1994, **27**, 435–436.
68 G. M. Sheldrick, in *SHELXL97*, University of Göttingen, Germany, 2008.